

# **Engineered Allosteric Regulation of Protein Kinases by Light**

**By**

**MARK SHAAAYA**

**B.Sc. Biochemistry, Lebanese University, 2008**

**THESIS**

Submitted as partial fulfillment of the requirements for the degree of Doctor of Philosophy in  
Cellular and Molecular Pharmacology in the Graduate College of the  
University of Illinois at Chicago, 2021

Chicago, Illinois

Defense Committee:

Dr. Andrei Karginov, Advisor and Chair

Dr. Viswanathan Natarjan, Co-advisor

Dr. Yulia Komarova

Dr. Richard Minshall

Dr. Andrius Kazlauskas, Physiology and Biophysics

## **DEDICATION**

I dedicate this work to my grade-school mathematics teacher, Mr. Jamal Maatouk, and my high-school Physics teacher, Mrs. Janet Eid. Their hard work and continuous strive to provide us with the best education possible greatly contributed to my interest in science at a young age and academic advancement.

## ACKNOWLEDGEMENTS

I am grateful to my advisor, Dr. Andrei Karginov for his excellent mentorship. His constant guidance sharpened my critical thinking skills and was indispensable for the completion of this work. I would also wish to thank my co-advisor, Dr. Viswanathan Natarajan, for his continuous support throughout my training years, and during the two years under his direct supervision. In his lab, I was trained to study the endothelial barrier function and wrote my first grant proposal under his mentorship. I would also wish to extend my gratitude to my research committee members, Dr. Yulia Komarova, Dr. Richard Minshall, and Dr. Andrius Kazlauskas for their insights and constructive criticism that helped improve the quality of this work.

A number of people whom we collaborated with were extremely helpful, namely Dr. Pradeep Kota from UNC, Anastasia Zhurikhina and Dr. Denis Tsygankov from Georgia Institute of Technology and Emory University, Dr. Jason E-Conage-Pough, Dr. Cameron T. Flower, and Dr. Forest M. White, from Massachusetts Institute of Technology, and Dr. Jalees Rehman and Dr. Young-Mee Kim from UIC.

I am also grateful for the past and current lab members from whom I have learned a lot during our productive lab meetings and casual daily chats. They have made the lab environment a happy place to be in every day during all my time in the program.

Finally, this work could not have been possible without the endless support and trust of my partner Felisha Gonzalez, my parents, and two sisters.

## CONTRIBUTION OF AUTHORS

Chapter I introduces my dissertation question. Chapter II is adapted from a literature review (Mark Shaaya, Jordan Fauser, & Andrei V. Karginov, 2020; Optogenetics, the art of Illuminating complex signaling pathways, accepted in the Physiology journal), that is a result of a teamwork between me, my colleague Jordan Fauser, and my advisor Dr. Andrei Karginov. In this chapter, I introduce optogenetics in the field of cell biology and go over recent approaches based on a thorough literature search. I describe the rationale behind their development and highlight their major advantages and limitations. Chapter III, IV, and V includes a manuscript that is currently in revisions (Shaaya M, *et al.* 2020; Light-Regulated Allosteric Switch Enables Temporal and Subcellular Control of Enzyme Activity. eLife). These three chapters describe the bulk of my work in the Karginov lab, of which I was its major driver. This work could not have been made possible without the contributions of my lab mates and collaborators, whom I was delighted to work with. Vincent Huyot was the person to initiate the project before I join the Karginov lab. Jordan Fauser in collaboration with Dr. Pradeep Kota from UNC performed the molecular dynamics modeling studies presented here. Martin Brennan, Jacob Matsche, and Shahzeb Khan contributed to the molecular biology and biochemical assays. Anastasia Zhurikhina and Dr. Denis Tsygankov, from Georgia Institute of Technology and Emory University, performed the analysis of cell-edge velocity. Dr. Jason E-Conage-Pough, Dr. Cameron T. Flower, and Dr. Forest M. White, from Massachusetts Institute of Technology, performed the mass spectrometry experiments and analysis.

## TABLE OF CONTENTS

<b><u>CHAPTER</u></b>	<b><u>PAGE</u></b>
I. INTRODUCTION .....	1
A. Statement of Hypothesis .....	3
B. Significance of Study .....	4
II. LITERATURE REVIEW .....	5
A. Optogenetics .....	5
1. Photoreceptors .....	5
a. Blue-light Photoreceptors.....	6
b. Red-light Photoreceptors .....	6
B. Optogenetic Approaches .....	7
1. Utilization of Photoreceptor Dimerization .....	8
a. Subcellular Localization .....	8
i. Targeting a Protein to Specific Region .....	9
ii. Targeting a Protein to Different Subcellular Compartments .....	11
iii. Light-Induced Asymmetric Signaling .....	13
2. Protein-Protein Interaction .....	15
i. Protein Interaction with Downstream Effectors.....	15
ii. Protein Dimerization.....	17
iii. Split-protein Reassembly .....	19
3. Allosteric Regulation .....	22
4. Regulation by Steric Interference .....	25
III. EXPERIMENTAL PROCEDURES .....	29
A. Molecular Dynamics Modeling .....	29
B. Amino Acid Sequence of LightR .....	29
C. Molecular Biology .....	30
D. Antibodies, Chemical Reagents and Cell Lines .....	30
E. Expression of Engineered Constructs .....	31
F. In vitro Kinase Assay .....	31
G. Biochemical Characterization of LightR kinases .....	32
H. Characterization of LightRCre .....	33
I. Production of LightR-Src HeLa Stable Cell Line .....	33
J. Mass Spectrometry .....	34
1. Sample Preparation .....	34
2. Phospho-tyrosine Enrichment and Mass Spectrometry Analysis .....	34
K. Cell Imaging and Image Analysis .....	37
1. Sample Preparation and Imaging Hardware.....	37
2. Cell Spreading and Protrusive Activity Analysis .....	37

## TABLE OF CONTENTS (continued)

<b><u>CHAPTER</u></b>	<b><u>PAGE</u></b>
3. Local Blue Light Stimulation .....	38
4. Polarity Index Calculation .....	38
5. Centroid Shift .....	38
6. Quantification of Cell Edge Dynamics.....	40
 IV. RESULTS .....	 43
A. Design of LightR Domain.....	43
B. Molecular Dynamic Studies suggests LightR is an Allosteric Switch .....	45
C. Blue Light Activates LightR-Src.....	49
D. Cells expressing LightR-Src Undergo Broad Phosphorylation Events Upon Light Illumination .....	52
E. LightR-Src Reveals Downstream Phosphorylation Temporal Dynamics .....	56
F. LightR-Src Activation is Reversible .....	59
G. LightR-Src Regulates Cell Morphology and Mimics Wild-type Src Localization .....	63
H. LightR-Src Activated at Subcellular Levels .....	67
I. Localized Src Activation Induces Waves of Membrane Protrusion .....	71
J. LightR Switch is Applicable to Other Kinases and Enzymes .....	73
 V. DISCUSSION .....	 84
 VI. FUTURE DIRECTION .....	 87
 VII. CITED LITERATURE.....	 89
 VIII. APPENDIX.....	 98
 IX. VITA .....	 100

## LIST OF FIGURES

<b><u>FIGURE</u></b>	<b><u>PAGE</u></b>
1. Targeting a protein of interest to its substrate location.....	10
2. Targeting a protein of interest to an organelle.....	12
3. Light-induced asymmetric signaling.....	14
4. Dissecting signaling pathways .....	16
5. Light-induced dimerization .....	18
6. Split-protein reassembly .....	21
7. Allosteric regulation .....	24
8. Regulation by steric interference.....	28
9. Polarity index and centroid shift .....	39
10. VVD photoreceptor and LightR design .....	44
11. LightR-Src molecular dynamics.....	46
12. Cross correlation maps of dark and lit states of LightR-Src .....	48
13. Characterization of LightR-Src .....	50
14. Principle component analysis .....	53
15. STRING biological network analysis .....	55
16. Temporal changes in protein phosphorylation induced by LightR-Src activation .....	57
17. Reversibility of LightR- and FastLightR-Src.....	60
18. Cycles of activation/inactivation of FastLightR-Src.....	62
19. Reversible and repetitive regulation of cell morphology by FastLightR-Src.....	64
20. Reversible and repetitive translocation of LightR-Src.....	66
21. Local regulation of FastLightR-Src at a subcellular level.....	68

## LIST OF FIGURES (continued)

<b><u>FIGURE</u></b>	<b><u>PAGE</u></b>
22. Local translocation of FastLightR-Src to focal adhesions.....	70
23. Localized Src activation induces waves of membrane protrusion .....	72
24. Conserved catalytic domain of kinases.....	74
25. Regulation of LightR-Abl and LightR-bRaf .....	76
26. Inactivation kinetics of LightR-bRaf and FastLightR-bRaf.....	78
27. Reversible and repetitive activation of FastLightR-bRaf .....	80
28. LigthR-Cre design and function.....	82



## LIST OF ABBREVIATIONS

Abl	Abelson tyrosine kinase
AD	Activation domain
AKT	Also known as PKB or Protein kinase B
Arp	Actin-related proteins
AsLOV2	LOV2 domain of Avina Sativaphototropin1
CAGE-prox	Computationally aided and genetically encoded proximal decaging
Cas	Crk-associated substrate
Cas9	CRISPR associated protein
Cdc42	Cell division control protein 42 homolog
CIBN	CRY-interacting basic helix–loop–helix protein 1
Cre	Causes recombination
CRY2	Cryptochrome 2
DBD	DNA binding domain
DNA	Deoxyribonucleic acid
DTT	Dithiothreitol
EGF	Epidermal growth factor
ERK	Extracellular signal-regulated kinase
FACS	Fluorescence activated cell sorting
FAD	Flavin dinucleotide
FAK	Focal adhesion kinase
Fe-NTA	Ferric nitrilotriacetate
FMN	Flavin mononucleotide

## **LIST OF ABBREVIATIONS (continued)**

FRET	Förster resonance energy transfer
GEF	Guanine nucleotide exchange factors
GFP	Green fluorescent protein
GTP	Guanosine triphosphate
GUI	Graphical user interface
HCD	Higher-energy collisional dissociation
HEK	Human embryonic kidney
iCre	Codon-improved Cre recombinase
iLID	Improved light inducible dimer
IMAC	Immobilized metal affinity chromatography
IP	Immuno-precipitation
LAD	Light activated dimer
LADC	Light activated dimer component
LANS	Light-activated nuclear shuttle
LC-MS	Liquid chromatography–mass spectrometry
LED	Light-emitting diode
LEXY	Light-inducible nuclear export system
LightR	Light regulated
LINus	light-inducible nuclear localization signal
LOV	Light-oxygen-voltage sensing
MD	Molecular dynamics
MEK	Mitogen-activated extracellular signal-regulated kinase

## **LIST OF ABBREVIATIONS (continued)**

MLC	Myosin light chain
MLCK	Myosin light chain kinase
NAMD	Nanoscale molecular dynamics
NCE	Normalized collision energy
NES	Nuclear export signal
NLS	Nuclear localization signal
nm	Nanometer
NMR	Nuclear magnetic resonance
NMWiz	Normal mode wizard
OpEn-Tag	Optogenetic endomembrane targeting
PA	Photo-activatable
PCA	Principal component analysis
PCB	Phycocyanobilin
PCR	Polymerase chain reaction
PDB	Protein data bank
pdDronpa	Photodimer Dronpa
PhyB	Phytochrome B
PI	Photoinhibitable
PI3K	Phosphatidylinositol 3-kinases
PIF	Phytochrome interacting factor
PKA	Protein kinase A
POI	Protein of interest
ProDy	Protein dynamics

## **LIST OF ABBREVIATIONS (continued)**

PSMs	Peptide spectrum matches
Rac1	Ras-related C3
Raf	Rapidly accelerated fibrosarcoma
RFP	Red fluorescent protein
RGS	regulator of G-protein signaling
Rho A	Ras homolog family member A
RMSD	Root-mean-square deviation
RNA	Ribonucleic acid
ROCK	Rho associate protein kinase
RTK	Receptor tyrosine kinase
SFK	Src family kinases
SOS	Son of sevenless
TF	Transcription factor
TMT	Tandem mass tag
trpR	Tryptophan repressor
UCSF	University of California, San Francisco
um	Micrometer
UV	Ultraviolet
VMD	Visual molecular dynamics
VVD	Vivid
WASP	Wiskott–Aldrich syndrome protein

## SUMMARY

Key biological processes in mammalian cells are regulated by protein kinases <sup>1</sup>. A single kinase can elicit distinct effects depending on its temporal activity dynamics as well as its subcellular localization <sup>2-5</sup>. This complexity of kinase signaling necessitates the development of tools enabling spatial and temporal control of their activity, which otherwise cannot be achieved with pharmacological and genetic methods. Here, I describe the development of an optogenetic tool, Light-Regulated (LightR) switch domain, that we engineered and utilized to achieve allosteric control of kinase activity.

Using tyrosine kinase Src as a model, we developed LightR-Src. We demonstrate an efficient regulation of the kinase with fast on-kinetics and we define signaling responses within seconds and minutes after LightR-Src activation. We show that the off-kinetics of LightR switch can be tuned by modulating its photoconversion cycle. Therefore, a fast cycling LightR-Src variant enables stimulation of transient pulses of Src activation in living cells. Local activation of LightR-Src in a cell induces local protrusions and cell polarization towards the light. Interestingly, continuous local Src activity stimulates recurring waves of protrusions mediated by Rho-associated protein kinase and myosin light-chain kinase. We demonstrate the broad applicability of this tool by achieving light-mediated regulation of Abl and bRaf kinases, as well as a different type of enzyme, Cre recombinase. Overall, we developed an optogenetic method that allows us to mimic dynamic protein activity at subcellular levels.

## **I. INTRODUCTION**

Dissection of biological processes is greatly aided by optogenetic methods that allow researchers to mimic and manipulate the function of individual proteins. Multiple broadly applicable approaches enable tight regulation of protein localization and interactions<sup>6-9</sup>. However, direct control of enzymatic activity remains a challenge. Only few existing strategies achieve direct regulation of enzymatic activity<sup>10-15</sup>, but they suffer from critical limitations. These methods either lack the ability to activate enzymes locally within a cell, or they are difficult to apply for the regulation of different enzymes<sup>10-15</sup>. We aimed to overcome existing challenges and developed an optogenetic approach that combines all advantages of light-mediated control and can be applied to a wide variety of proteins. An attractive strategy that can be harnessed for this purpose is the application of a rationally designed light-sensitive domain that can control protein activity allosterically. This protein-engineering approach offers several important advantages. It enables targeted regulation of one domain within a multidomain protein<sup>16</sup>. Regulation is achieved without sterically interfering between the catalytic pocket of the enzyme and its substrate. Also, allosteric switch domains are encoded into the targeted protein simplifying the application of the tool. However, existing strategies for allosteric regulation do not combine the features of broad applicability and local subcellular control of enzymes in one tool<sup>11, 14, 15, 17</sup>. Furthermore, existing allosteric switches lack tunable adjustment of their own kinetics, an important feature required for inducing different temporal dynamics of engineered signaling enzymes. Thus, we set out to develop an allosteric switch that can overcome these existing challenges.

Among many research targets, protein kinases represent an important family of enzymes that regulate many physiological functions. To ensure proper outcome, kinase activity is tightly

controlled in cells. Perturbations in the regulation of kinases often lead to pathological consequences<sup>1</sup>. Many kinases are used as therapeutic targets and significant research effort is directed towards uncovering their function in cells. These studies are challenging because a single kinase often induces drastically different responses depending on the location, level and timing of its activation<sup>2-5, 18</sup>. Furthermore, transient, sustained or oscillatory kinase activation can result in distinct outcomes. Therefore, interrogating kinase-mediated signaling requires approaches capable of mimicking complex spatiotemporal control of kinase activity down to the subcellular resolution. Traditional methods using genetic manipulation and small molecule inhibitors lack this level of regulation. Optogenetics, on the other hand, overcomes these limitations<sup>19</sup>. Some existing optogenetic tools regulate the dimerization or localization of kinases<sup>18, 20-23</sup>. These approaches control the catalytic activity only indirectly and cannot be applied to many kinases. On the other hand, some approaches employ light-sensitive caging or allosteric switches for the regulation of kinase catalytic domains<sup>10-12</sup>. However, these methods do not achieve subcellular control of activity and some of them cannot be applied to all kinases due to structural requirements<sup>10-12</sup>. Thus, the regulation of protein kinases by optogenetic methods remains a challenge.

## **A. Statement of Hypothesis**

To develop a light-regulated allosteric switch, we envisioned a clamp-like domain that can reversibly close in response to light and can be incorporated in an allosteric site in a protein of interest. We thought that this switch could be made possible by connecting two Vivid (VVD) photoreceptors, which dimerize in response to blue light. In the lit state, two VVD domains undergo a structural change and dimerize in an antiparallel fashion such that the N-terminus of one VVD domain and the C-terminus of the other are only 10 Å apart, acting like a closed clamp. However, in the dark state, the structural change of VVD is reversed and the N- and C-termini are far apart thereby acting like an opened clamp. We hypothesized that inserting this opened light-regulated clamp in an allosteric site of a constitutively active kinase will introduce a structural disruption to its catalytic domain, inactivating its function. However, closing the clamp with blue light will restore the catalytic domain active structure and thereby reactivate the kinase. To address this hypothesis, we started by performing molecular dynamic simulations of LightR-Src as a predictive measure of its success. We then engineered LightR-Src, expressed it and tested its activity in response to blue light in living cells.



**B. Significance of Study**

Here we developed an approach that overcomes limitations of existing optogenetic methods by employing an engineered light-sensitive switch domain that is genetically encoded and enables the allosteric regulation of kinase catalytic domains. With this method, we were able to achieve fast, specific, and tunable control of kinase activity in living cells using low intensity of blue light. Furthermore, this method enables reversible and repetitive activation of a kinase and provides local control of its activity at subcellular levels. Application of this tool allowed us to uncover temporal dynamics of phosphorylation-mediated signaling following short term (10 seconds) as well as prolonged activation of a kinase. Importantly, we show that this approach can be applied not only to different kinases but also to other enzymes.

## **II. LITERATURE REVIEW**

### **A. Optogenetics**

Optogenetic approaches are developed to allow for precise spatiotemporal manipulation of cellular events using light. This field was first employed in Neuroscience, when scientists exploited rhodopsin photoreceptors to control the membrane potential of neurons <sup>24, 25</sup>. This enabled precise control over the activity of individual neurons, facilitating the characterization of their distinct functions. Inspired by these approaches, the cell biology field witnessed an emergence of a variety of optogenetic tools to study cell signaling circuits, which I will be discussing further. Optogenetics in cell biology involves the genetic modification of proteins for the purpose of coupling their functional output with an optical input <sup>19</sup>. This offers an unprecedented flexibility for the temporal and spatial regulation of protein activity with light. The genetic modification often involves the utilization and incorporation of genetically encoded photoreceptors in the protein of interest.

#### **1. Photoreceptors**

Photoreceptors are naturally occurring proteins that enable organisms across multiple kingdoms to respond to light <sup>26</sup>. These receptors contain a chromophore moiety embedded in their core. Chromophores are photon absorbing non-protein pigments that change conformation in response to light. The photochemistry properties of chromophores determine the sensitivity of individual photoreceptors to certain wavelengths of light as well as its kinetics in responding to light <sup>26</sup>. Chromophores directly interact with surrounding residues in the structure of photoreceptors. Structural alterations in chromophores are amplified through allosteric networks to result in intramolecular conformational changes in the photoreceptor <sup>26</sup>. In some

photoreceptors, this change can result in its association with one molecule of the same protein to form a homodimer, or many molecules to form a homo-oligomer. Other photoreceptors associate with one molecule of a different protein to form a heterodimer or undergo an irreversible cleavage in response to light.

A variety of photoreceptors have been discovered and they are generally divided between blue-light and red-light photoreceptors, depending on the wavelength of light they respond to.

**a. Blue-light Photoreceptors**

Light-oxygen-voltage sensing (LOV) domain derivatives and Cryptochromes are the most widely implemented photoreceptors in engineering light-regulated enzymes. These two classes of photoreceptors are desired for the following reasons. They respond to blue light, which is less phototoxic to living cells than the ultraviolet light. These photoreceptors spontaneously return to their basal state in the dark. They also have flavin mononucleotide (FMN) or flavin dinucleotide (FAD) as their chromophore, which is readily available in mammalian cells and therefore do not require exogenous supply. Therefore, due to these properties, the majority of optogenetic tools developed in cell biology utilize blue-light photoreceptors.

**b. Red-light Photoreceptors**

Phytochromes are the second most used class of photoreceptors, particularly the Phytochrome B/Phytochrome interacting factor (PhyB/PIF) heterodimer pair. This pair dimerizes in response to red light and dissociates when excited with far-red light, which makes it especially suitable for regulating optogenetic proteins in thick tissues or in *in-vivo* models since red-shifted light is more penetrative than blue-shifted light. However, phytochromes require

phycocyanobilin (PCB) or phytochromobilin as a chromophore, and mammalian cells do not synthesize these molecules. Therefore, when using optogenetic tools that incorporate phytochromes in their design, the chromophore must be supplemented exogenously, which can be technically inconvenient, especially in *in-vivo* experiments. To overcome this limitation, Aoki group designed a vector that when expressed in mammalian cells, the mitochondria synthesizes intracellular PCB at concentrations sufficient to make the PhyB/PIF system functional without exogenous supply of the chromophore <sup>27</sup>.

## **B. Optogenetic Approaches**

In cells, information is relayed in the form of complex and dynamic signaling events that translate into various cellular functions <sup>28</sup>. One protein molecule can mediate different signaling outputs depending on its binding partners <sup>29</sup>. While the identity of binding partners is critical in determining the signaling outcome of a protein, its temporal activity dynamics can also dictate its function <sup>2, 4, 5</sup>. Furthermore, signaling events are compartmentalized and occur at subcellular levels <sup>30</sup>. Therefore, it has become clear that a thorough investigation of signaling molecules requires the ability to target them to specific binding partners and mimic their complex spatiotemporal dynamics. This challenging task is greatly aided by innovative tools for interrogating cell signaling with physiologically relevant dynamics. While generally useful, commonly used methods of gene silencing or knockout as well as diffusible activators and inhibitors act on cells globally and irreversibly. Therefore, these applications lack the intricate control needed to parse out complex signaling events. In an attempt to develop tools that overcome these limitations, cell biologists adapted optogenetic approaches from the neuroscience field and developed them further to manipulate cellular signaling.

## **1. Utilization of Photoreceptor Dimerization**

One aspect that determines the function of signaling molecules is their formation of specific protein complexes within certain subcellular compartments. However, investigating the role of protein localization and interaction in signaling has proven difficult using the classic molecular biology and pharmacological approaches. Optogenetics provides a modular toolbox to reconstruct and study these interactions even at subcellular levels. Photoreceptors exhibit features that are employed to induce selective regulation of a protein of interest. In response to light, some photoreceptors undergo structural changes, which lead to the formation of a dimer, or what I will refer to hereafter as light activated dimer (LAD). This property is utilized in regulating subcellular localization, protein-protein interaction, transcription, and protein activation; as discussed below.

### **a. Subcellular Localization**

Targeting a protein of interest to different cellular compartments allows researchers to investigate its specific local signaling. Cry2-CIBN photoreceptor dimer is the most widely used LAD system for subcellular targeting applications. However, recent research demonstrated that other LAD pairs, such as iLID/SspB or VVD magnets, offer improved dimerization and dissociation kinetics<sup>31</sup>. As a general design, the protein of interest is fused to one component of the dimer system (LADC1) while the other component (LADC2) is localized to the targeted subcellular compartment<sup>32-34</sup>. Therefore, the engineered protein is diffuse throughout the cell in the dark, and in light the photoreceptor that is fused with it dimerizes with the photoreceptor at the desired target, thereby localizing the protein to the target of interest. This general approach can be used to: (a) localize the protein to the site of its substrate or interacting partner, (b)

localize the protein to different subcellular compartments, and (c) asymmetrically target the protein to one side of the cell using focused light.

#### **i. Targeting a Protein to Specific Region**

A protein of interest can be targeted to a region containing its substrate or signaling partners to induce signaling. In the dark, this protein that is fused to a photoreceptor will be diffuse throughout the cell and unable to induce signaling. Stimulation with light targets the protein to the site rich in its substrate or signaling partners (Figure 1). This provides direct control over the initiation of signaling pathways and thus an elegant approach to study their dynamics.

This technique has been applied to regulate phospholipid signaling and metabolism at the plasma membrane through specific targeting of inositol-5-phosphatase, PI3K, or AKT <sup>35</sup>. Idevall-Hegran et al. used CRY2-CIBN system to target inositol-5-phosphatase to the plasma membrane <sup>36</sup>. The plasma membrane is rich in PI(4,5)P<sub>2</sub>, an inositol-5-phosphatase substrate. Therefore, after targeting the phosphatase to the plasma membrane, it could act on its substrate, thus regulating phospholipid signaling with tight temporal and spatial control <sup>36</sup>. This approach has also been used to activate GTPases by targeting their specific guanine nucleotide exchange factors (GEFs) to the plasma membrane, where GTPases are innately localized <sup>18, 37-39</sup>. Toettcher et al, using the PhyB/PIF dimer system, targeted SOS to the plasma membrane to induce Ras activation and investigate the role of Ras/ERK dynamics in cell fate determination <sup>18</sup>. Meanwhile, other groups have used the blue light dimer system iLID/SspB to target specific GEFs for Rac1, CDC42 and RhoA GTPases to the plasma membrane <sup>39</sup>.

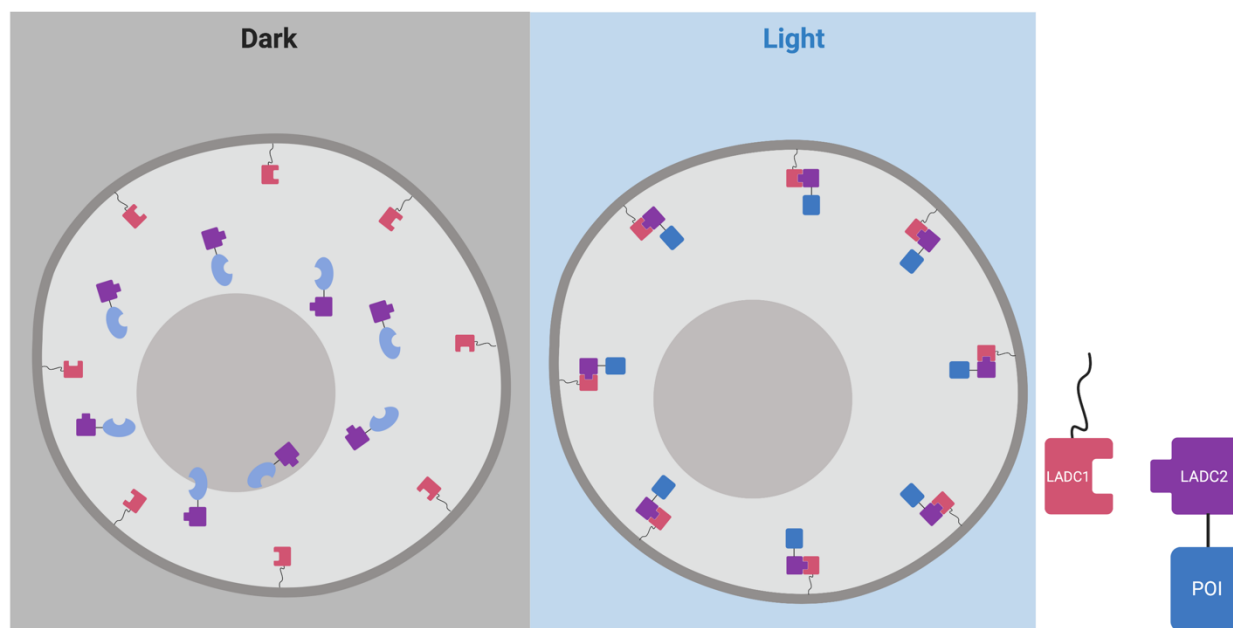


**Figure 1: Targeting a protein of interest to its substrate location.** In this illustration, the substrate of the protein of interest (POI) is innately located at the plasma membrane. To target the POI to the cell membrane, one can fix a LADC1 to the plasma membrane by fusing it with a membrane localization signal. In response to light, the diffuse POI fused with LADC2 will translocate to the cell membrane and initiate signaling through its substrate.

## **ii. Targeting a Protein to Different Subcellular Compartments**

Proteins can exhibit different signaling based upon their subcellular localization. Most techniques used for the interrogation of signaling act globally on cells making it impossible to study signaling events in different cellular compartments. Using optogenetics methods, one can distinctly interrogate signaling pathways initiated by a protein of interest at any subcellular compartment. This is achieved by tagging a protein that is naturally localized on a targeted organelle with one LAD component. The second LAD component is fused to the protein of interest, allowing for the relocation of the protein to the targeted organelle through light induced dimerization of the LAD components (Figure 2). This targeting approach can be applied to investigate different signaling impacts of an active protein at different locations, such as the study conducted with Protein Kinase A (PKA). By targeting the catalytically active PKA subunit to the outer mitochondrial membrane and plasma membrane, researchers defined compartment-specific PKA signaling <sup>40</sup>. The applications of this technique were expanded with the development of OpEn-Tag (optogenetic endomembrane targeting); a customizable toolbox for targeting proteins to various compartments within the cell <sup>41</sup>. This two-component system contains a variety of endomembrane targeting peptides fused to an mCherry labeled CBIN and a protein of interest fused to CRY2. To demonstrate the applicability of the OpEn-Tag system, the researchers selectively targeted AKT1 to the plasma membrane, and inner and outer mitochondrial membranes. In doing so, they determined the plasma membrane has a significant role in AKT1 activation <sup>41</sup>.



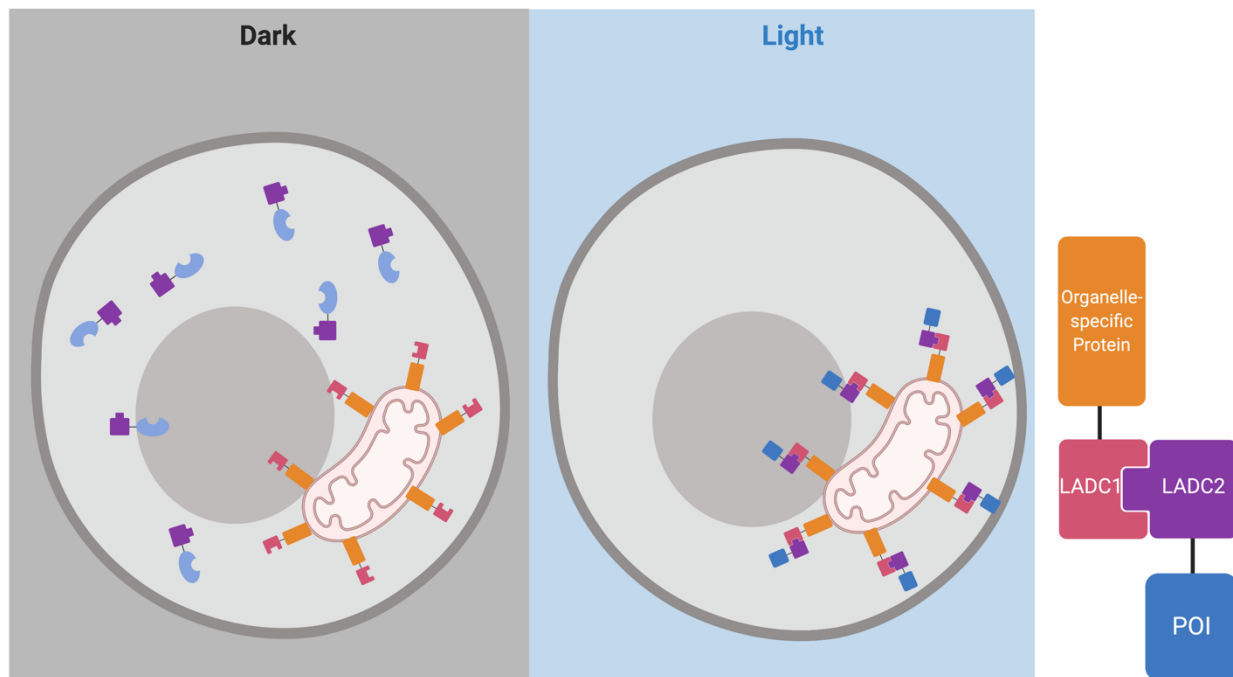


**Figure 2: Targeting a protein of interest to an organelle.** A protein known to be specifically localized at an organelle can be fused with LADC1. In response to light, a POI fused to LADC2 translocates to the organelle.

### **iii. Light-induced Asymmetric Signaling**

Some cellular functions require asymmetric signaling activity, especially for polarized cellular behaviors such as migration. This can be mimicked utilizing a similar approach as those discussed above; the protein is fused to LADC1 while LADC2 is tagged with a specific localization signal. The application of light results in the translocation of the protein to the membrane of interest. Spatial regulation is further enhanced by using a focused beam of light or a gradient of light by which researchers can illuminate one side of the cell to stimulate asymmetrical signaling (Figure. 3), thereby inducing polarized cellular behaviors<sup>30, 42-44</sup>. O'Neil and Gautam employed this strategy to dissect the role of G-protein signaling gradients in cells<sup>42</sup>. Using a membrane localized CIBN, a negative regulator of G-protein signaling (RGS) fused to CRY2 was targeted to the membrane following blue light illumination. By applying focused light to only one side of the cell, the targeted inhibition of G-protein signaling was limited to the illuminated side of the cell. Combining this with global chemical activation of G-protein signaling, the cell developed polarized signaling with the dark side actively signaling while the lit side being inhibited. This mimicked a G-protein signaling gradient, which specified its role in immune cell migration<sup>42</sup>. In another example, Graziano et al. employed local recruitment of PI3K to define the role of sustained PIP3 signaling at the leading edge of a migrating neutrophil<sup>45</sup>. Using localized illumination, they targeted the PIF-tagged PI3K to a membrane bound PhyB on one side of the cell generating a highly polarized and sustained PIP3 production. They demonstrated that PIP3 signaling is sufficient to induce cell polarization and migration. Importantly, this study found that sustained PIP3 signaling induces only a transient Rac activation through a mechanism where actin assembly and ArhGAP15 signaling trigger a negative feedback loop downregulating Rac1.

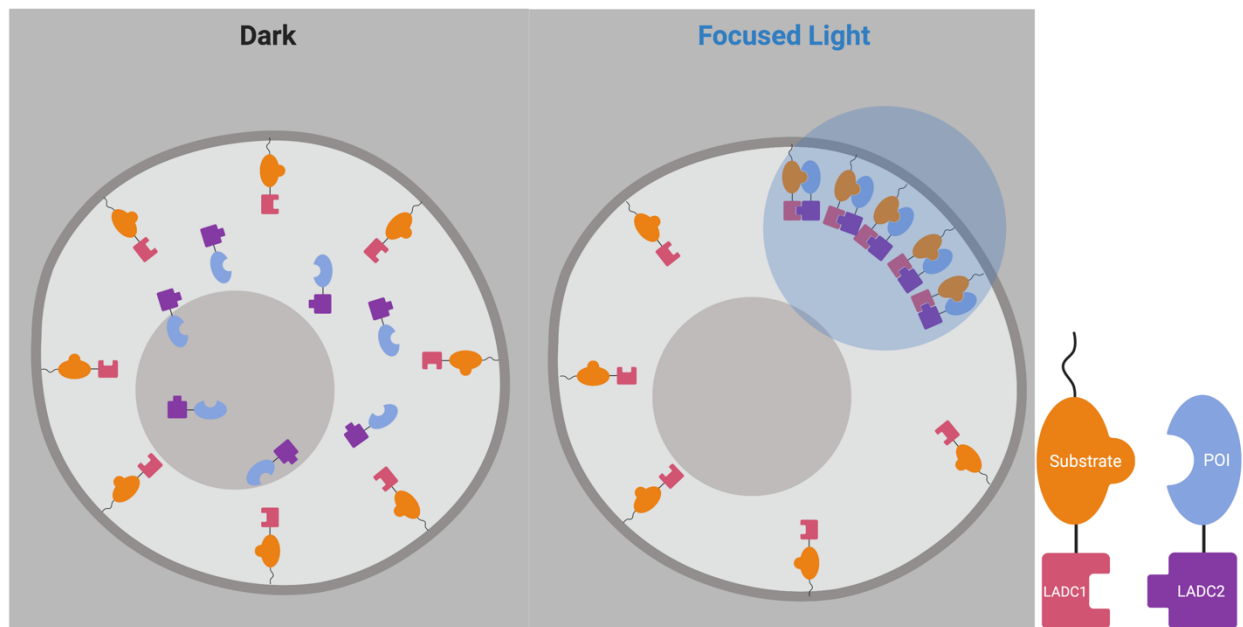


**Figure 3: Light-induced asymmetric signaling.** Asymmetric signaling can be mimicked using focused beam of light to activate a signaling pathway in one side of the cell.

## **2. Protein-Protein Interaction**

Protein-protein interaction and the formation of signaling complexes are critical in regulating and propagating signals within cells. One signaling molecule can induce different cellular responses depending on the identity of its downstream signaling partner. While point mutations can be used to alter protein-protein interactions, they lack temporal regulation and can affect unintended signaling partners. Light induced dimerization or oligomerization of photoreceptors fused to proteins of interest enables dynamic regulation of protein-protein interactions as well as specific protein clustering.

### **i. Protein Interaction with Downstream Effectors**

Signaling molecules often interact with multiple signaling partners. Therefore, activating one protein can lead to parallel stimulation of multiple downstream signaling pathways. To dissect and investigate the unique function of one of these pathways is challenging. Using optogenetics, it is possible to activate a single downstream pathway without affecting the rest. This is achieved by fusing a protein of interest to one LAD component and fusing a specific signaling partner to the other component. In response to light, the protein fused with the LAD component will solely bind and activate that particular signaling partner, eliciting the specific downstream effects of that protein-protein interaction (Figure 4). This technique was applied to interrogate the role of Cdc42 interaction with a specific effector, WASP, in actin assembly. Using the heterodimerizing photoreceptor pair PhyB and PIF fused to Cdc42 and WASP respectively, the researchers were able to induce Cdc42 and WASP interaction following red-light exposure. This interaction was sufficient to induce the formation of the Arp2/3 complex and actin assembly <sup>46</sup>.

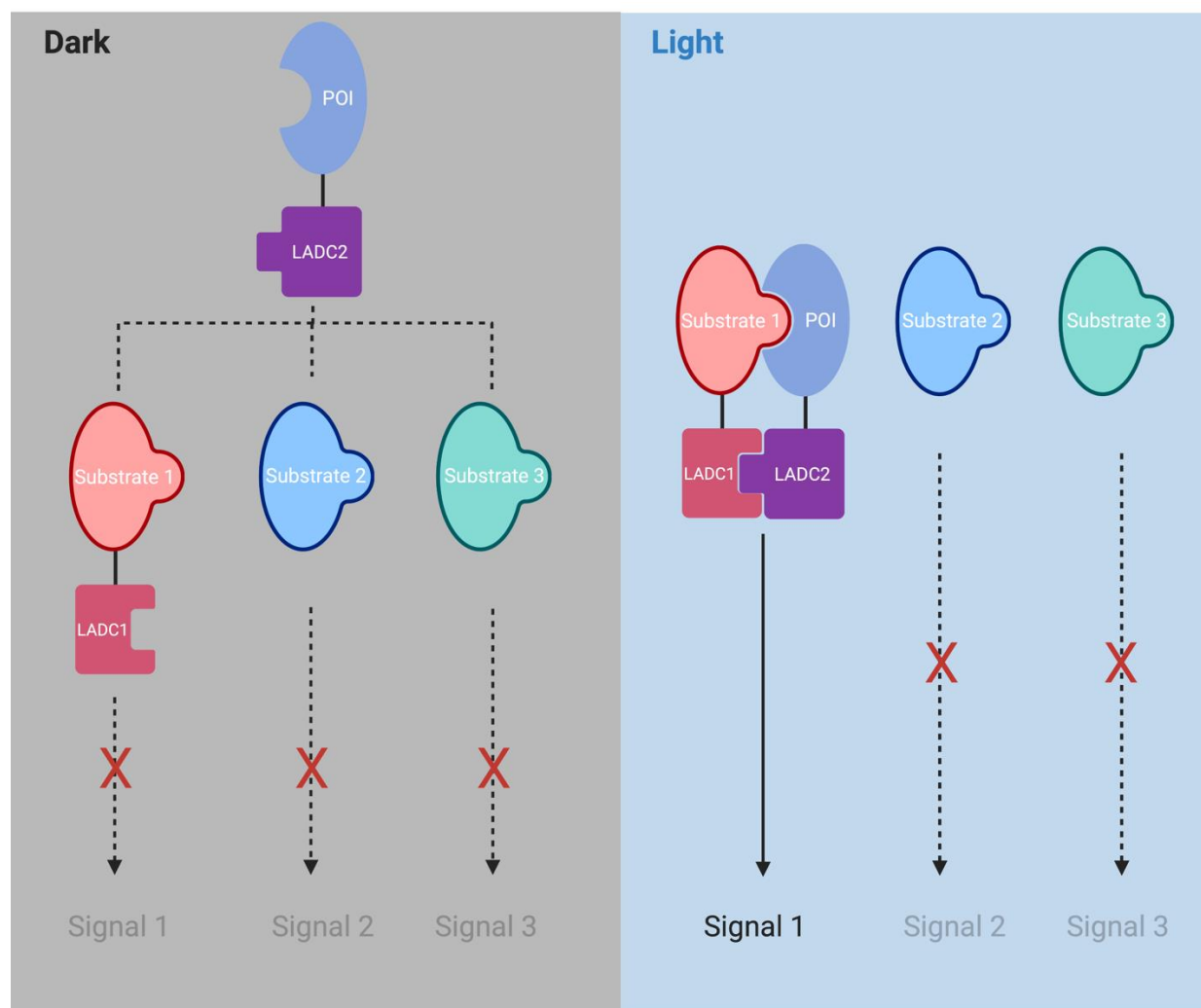


**Figure 4: Dissecting signaling pathways.** A POI may activate multiple downstream signaling pathways. To activate only one pathway, a POI can be targeted to one substrate of interest using a LAD system.

## ii. **Protein Dimerization**

While optogenetic regulation of protein-protein interaction has been used for a variety of signaling molecules, it has been particularly beneficial in studying receptor tyrosine kinases (RTKs) and other kinase dimers. Different subtypes of RTKs often can homo-or hetero-dimerize upon the interaction with specific ligands. This dimerization results in the trans-phosphorylation and activation of the RTK. Each combination of dimers can mediate different signaling outcomes. Optogenetics allowed researchers to control dimerization of RTKs independently of ligand binding, and thus interrogate specific signaling outputs of unique dimer pairs with spatial and temporal control (Figure 5). This approach was used to induce homodimerization and activation of Fibroblast Growth Factor Receptor, Epidermal Growth Factor Receptor, and c-MET receptor<sup>21, 47-49</sup>. An additional level of regulation was achieved using the homo-oligomerization property of CRY2 to cluster active RTK dimers into physiologically relevant signaling hubs<sup>48</sup>. This enhanced RTK signaling while avoiding artifacts resulting from over-expression or hypersensitivity to the ligand. These oligomerization approaches are not limited to RTKs and have been applied to RhoA, LRP6, and Rab GTPases to enhance their signaling pathways beyond what can be achieved with ligand stimulation<sup>48, 50</sup>. Light-regulated dimerization was also employed to interrogate function of non-receptor kinases<sup>23, 47</sup>. Optogenetic control of b-Raf and c-Raf homo-and hetero-dimers demonstrated that the effect of clinically approved Raf inhibitors on signaling depends on the type of the dimer pairs<sup>49</sup>.

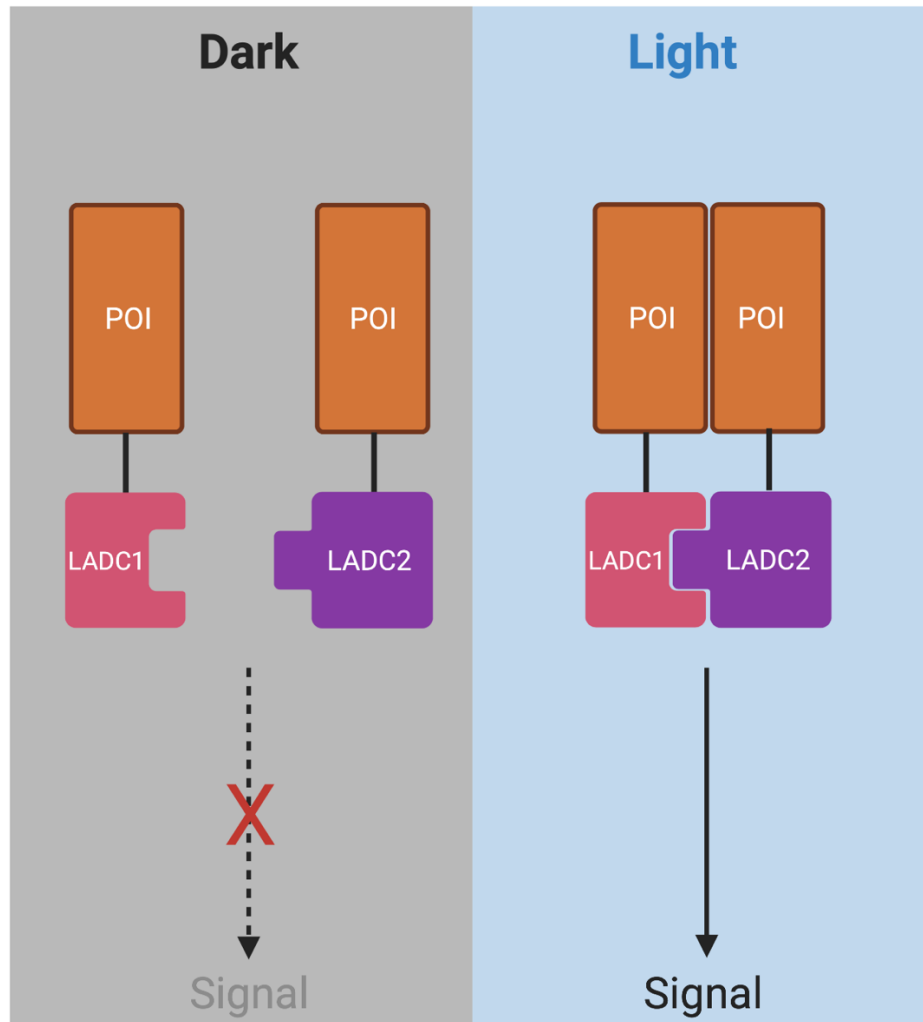


**Figure 5: Light-induced dimerization.** Dimerization can be a prerequisite for some proteins to get activated and signal. Dimerization, and therefore activation, can be regulated by light through fusing the protein monomers with a LAD system.

### **iii. Split-Protein Reassembly**

The fundamental realization that nonfunctional fragments of a protein can reassemble to form a functional protein <sup>51-53</sup> led to the utilization of this property to develop reporters for studying protein-protein interaction and tools for regulating protein activity <sup>54-57</sup>. Importantly, non-covalent reconstruction of inactive protein fragments using photo-dimers has proven to be successful in modulating protein function (Figure 6) <sup>58</sup>. Magnets and Cry2-CIB1 are the commonly used hetero-dimer systems in engineering optogenetic split-protein reassembly tools <sup>59-62</sup>.

For instance, CRY2-CIB1 dimerization system was implemented for light-regulated genetic manipulation through engineering DNA editing enzymes. The Tucker lab created split Cre recombinase using CRY2-CIB and demonstrated its in vivo functionality in rodent brains <sup>63</sup>. <sup>64</sup>. Sato group also developed a photoactivatable split Cre recombinase (PA-Cre) using magnets dimerization system <sup>65</sup>. PA-Cre was capable of genetically recombining DNA in a mouse organ in response to external LED light. Following this strategy, the same group developed a photoactivatable split Cas9 (paCas9) <sup>66</sup>, and later engineered the newly emerged RNA-guided DNA nuclease, Cpf1 <sup>67</sup>.

Recently, a novel tool of optogenetically activated intracellular antibody (optobody) based on split-protein reassembly was developed using magnets system <sup>9, 68</sup>. Intracellular antibodies (intrabodies) are small antibody fragments that bind and neutralize endogenous proteins. Therefore, using optobodies, one can control the affinity of intrabodies in living cells in a spatiotemporal manner. This provides great means to manipulate and define the role of endogenous proteins. The tool applicability was demonstrated by inhibiting endogenous gelsolin and beta-2 adrenergic receptor <sup>68</sup>.



The red/far-red PhyB/Pif dimer system has also been implemented to engineer optogenetic split transcription factors (TFs) <sup>69, 70</sup>. Typically, a TF is split into its DNA binding domain (DBD) and activation domain (AD), each fused with one LAD component. Upon light irradiation, the DBD and AD are brought into close proximity through the LAD system, and subsequently gene expression is initiated <sup>69</sup>. The DBD can be customized to target any gene of interest <sup>59, 60, 62</sup>; the AD can also be replaced with a repression domain to induce silencing of a target gene <sup>59</sup>.

Although optogenetic split-protein reassembly is proven to work, this approach has its own challenges. Split proteins can spontaneously reassemble, depending on the split site selected, resulting in undesired basal activity of the protein in the dark state. Fragments could also fail to fully reassemble, thus preventing effective activation. Therefore, finding the optimal splitting site in a protein is subject to extensive trial and error. Recently, the Dokholyan group developed a server to predict and rank potential splitting sites for regulating a protein of interest with light or cell-permeable ligands ([spell.dokhlab.org](http://spell.dokhlab.org)) <sup>71</sup>, to aid in developing such tools.

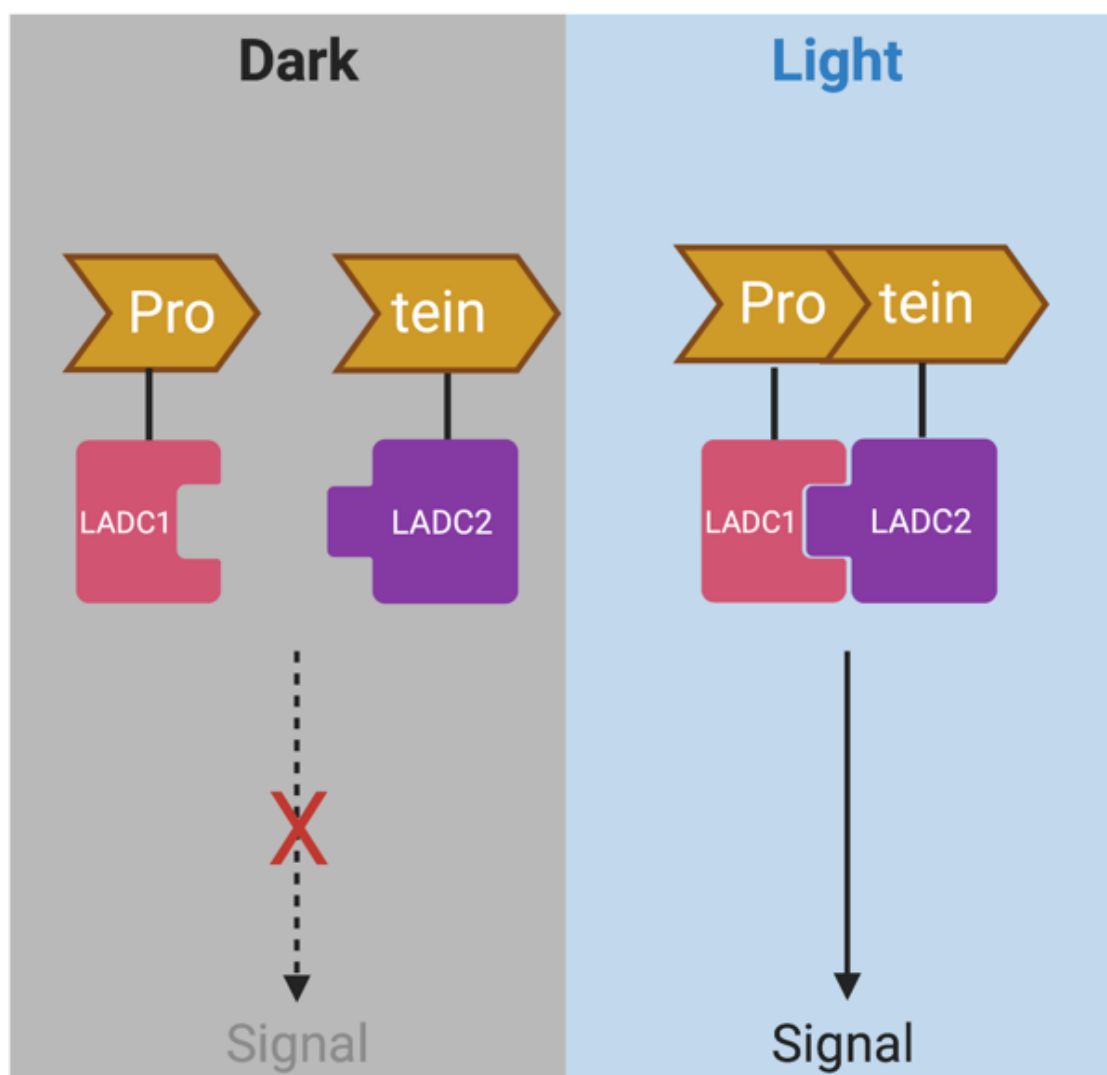


**Figure 6: Split-protein reassembly.** Two inactive protein fragments fused with LAD components can reassemble and recover the protein activity in response to light.

### 3. Allosteric Regulation

Allosteric regulation of enzymes is desirable for studying catalytic effects of proteins whose dimerization is not a prerequisite for their activation. Proteins that are engineered to be regulated allosterically retain their native subcellular localization, intermolecular interactions, and access to their substrates. Moreover, once an enzyme of interest is engineered to be allosterically regulated, the approach can be generally applied to other enzymes that share similar catalytic structure.

Allosteric regulation was inspired by the notion that any alteration that disrupts the catalytic site of a protein results in its deactivation<sup>72</sup>. One common mode of action for photoreceptors is undergoing a conformational change in response to light. This property of photoreceptors was utilized to develop optogenetic tools where a light-regulated domain is structurally coupled to the catalytic site of the protein<sup>73</sup> (Figure 7). Using a crystal structure or model of the protein of interest, a suitable allosteric insertion site is selected to be distant, yet structurally coupled, to the catalytic residues. Ideal insertion sites for allosteric switches often represent exposed loops within the catalytic domain<sup>74, 75</sup>. Since protein structure is directly related to its function, inserting a light regulated domain in these loops can control the catalytic activity of the protein by switching the catalytic site's structure between active and inactive state by toggling the light.

An elegant study by Hahn group used AsLOV2 domain to create an allosteric light switch to reversibly inhibit proteins in response to blue light<sup>75</sup>. AsLOV2 was inserted in a previously characterized allosteric loop in Src kinase<sup>76</sup>. Since the N- and C-termini of AsLOV2 are just 10 Å apart in the dark, they hypothesized that inserting AsLOV2 in the allosteric loop of a constitutively active Src should not perturb its structure and hence its function. However, when

the N and C termini of AsLOV2 separate in response to blue light, it introduces disorder in the coupled catalytic domain resulting in deactivation of Src. This approach generated a photoinhibitable Src, or PI-Src <sup>75</sup>. To demonstrate its generalizability, they applied the method to GTPases and GEF enzymes to produce PI-GTPase and PI-GEF, respectively. A similar approach was applied to engineer a photoactivatable bacteriophage T7 RNA polymerase using VVD photoreceptor <sup>77</sup>. In another example, AsLOV2 domain was employed to engineer a photoactivatable Escherichia coli trp repressor (trpR) <sup>78</sup>.

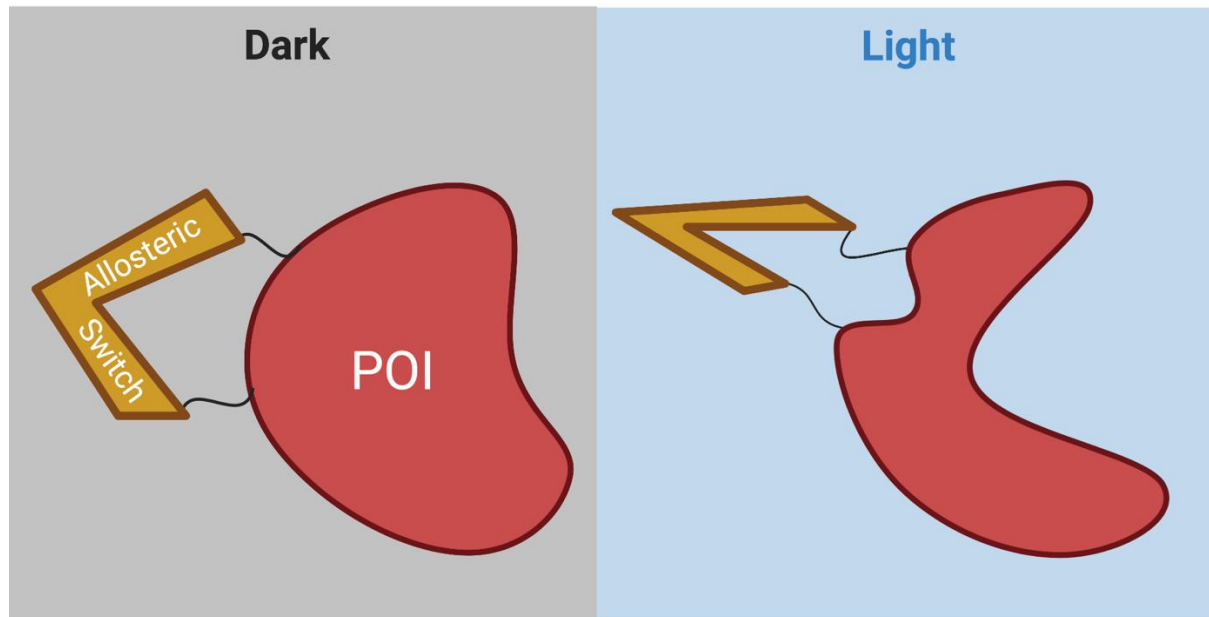


**Figure 7: Allosteric regulation.** A photoreceptor inserted in an allosteric site can act as a switch to regulate a protein's activity by light.

#### 4. Regulation by Steric Interference

Steric interference, when implemented in optogenetics, is referred to as photo-caging. This approach uses a light-sensitive group to cage a peptide or a region of interest in a protein, thereby sterically occluding it and blocking its function. The function is then recovered by uncaging the region in response to a specific wavelength of light (Figure 8). These photo-caging tools most commonly utilize AsLOV2 photoreceptor, but I will also discuss a tool that use pdDronpa1, which is engineered from the green fluorescent protein DronpaN145 to photocage catalytic sites. Furthermore, in addition to using photosensory protein domains, photo-caging was made possible using light-sensitive caged artificial amino acids, which will also be addressed here.

LOV2 domain from *Avena sativa* phototropin 1 (AsLOV2) has been extensively utilized as a photocage due to the reversible structural change it undergoes in response to blue light. AsLOV2 structure is characterized by a C-terminal helix (J $\alpha$  helix) docked onto a compact core in the dark. In response to blue light, the J $\alpha$  helix undocks and becomes exposed. Protein engineers exploited this feature of AsLOV2 domain to cage peptides by incorporating them in the J $\alpha$  helix. In the dark, the peptide is masked which reduces the affinity to its binding partners. Blue light unmask the peptide, thereby restoring the affinity to its binding partner. This strategy was applied by two groups to generate light-inducible nuclear localization signal (LINus) and light-activated nuclear shuttle (LANS)<sup>79, 80</sup>. Both are tools that function to translocate proteins using light from the cytosol to the nucleus by incorporating a nuclear localization signal (NLS) in the J $\alpha$  helix of AsLOV2 domain. Similarly, this strategy was used to engineer a light-inducible nuclear export system (LEXY), by incorporating a nuclear export signal (NES) in the J $\alpha$  helix of AsLOV2<sup>81</sup>. Since transcriptional factors are generally sequestered in the cytosol in their inactive

state, and shuttle to the nucleus when active, light-regulated caging and uncaging of the NLS or NES motifs provides an effective method to regulate transcription within the cell <sup>80, 82, 83</sup>.

Peptide caging using AsLOV2 is not limited to the regulation of protein localization. Studies also utilized AsLOV2 to photocage inhibitory peptides to manipulate the activity of endogenous kinases (PKA and MLCK) by light <sup>84</sup>. AsLOV2 was also used for light-dependent colocalization <sup>85</sup>. By masking ipaA and SsrA peptides (using LOV-ipaA and LOV-SsrA) from their binding partners (vinculin and SspB), it was possible to induce their colocalization using light <sup>85</sup>. This method was also used to regulate protein degradation signal by adding a degron to the C-terminus of AsLOV2 <sup>86, 87</sup>. This allows for light induced degradation of the protein of interest simply by fusing it with the degron containing LOV domain.

Light-controlled steric hindrance of a catalytic site has been employed for the regulation of enzymatic activity. Lin group applied this approach to create photoswitchable kinases using the engineered photo-dimer pdDronpa, which dissociates in blue light and reassembles in violet light. pdDronpa is fused to the kinase such that the dimer encircles the catalytic pocket, sterically occluding the substrate binding when dimerized in blue light <sup>88</sup>. Once in violet light, the dimer dissociates; allowing the substrate to access the kinase catalytic pocket and subsequently be phosphorylated. This process is reversible and therefore provides temporal control over activity <sup>88</sup>. A similar strategy was later applied by Klaus Hahn's group to develop a photocage system named Z-lock <sup>89</sup>. Here, LOV and Zdk photodimer system, instead of pdDronpa, was utilized to cage the catalytic site of cofilin and  $\alpha$ TAT. This system is smaller in size relative to pdDronpa, facilitating engineering. Also, LOV and Zdk affinity is adjustable, making Z-lock a tunable system <sup>89</sup>.

Alternatively, a catalytic domain can be sterically blocked using a photo-caged amino acid. Recently, a strategy named ‘computationally aided and genetically encoded proximal decaging’ (CAGE-prox) was developed <sup>10</sup>. This approach incorporates an artificially caged amino acid in a position proximal to the catalytic region. This is sufficient to block the activity of the protein, until it is restored by uncaging the amino acid using UV light. This method has the advantage of using a small caged amino acid instead of bulky photo-domains, however, it is an irreversible tool and lacks subcellular regulation capabilities.



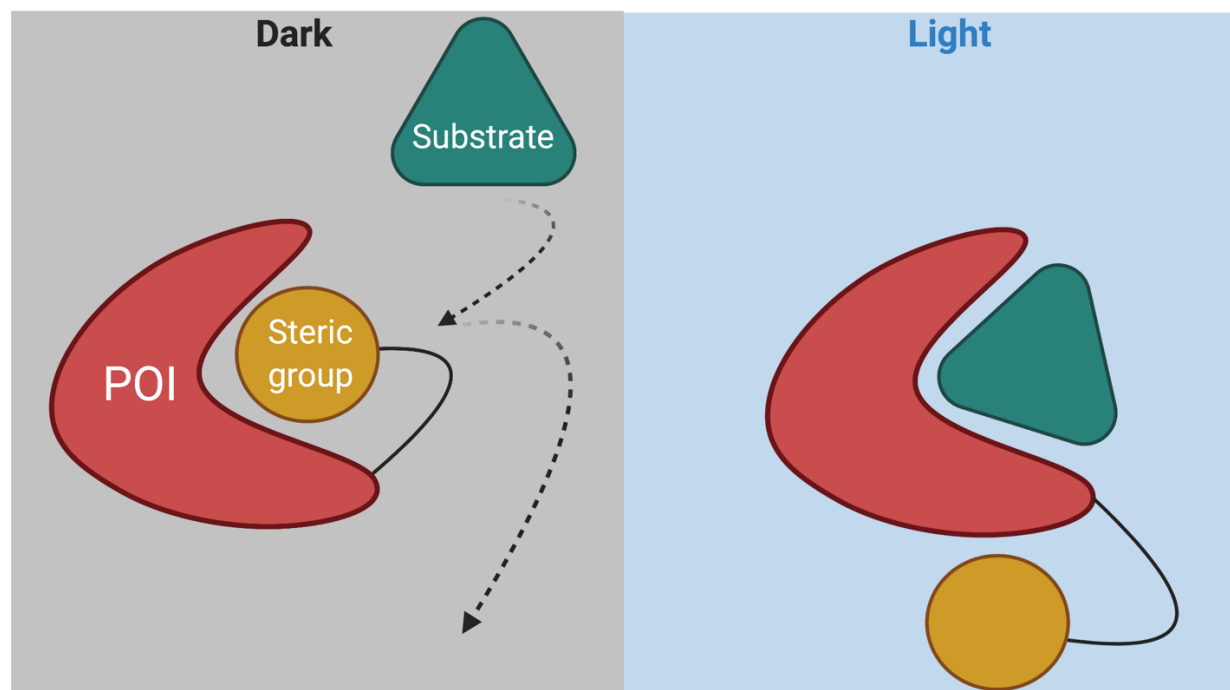


**Figure 8: Regulation by steric interference.** A photoreceptor or a photocaged group can be inserted in a POI in such a way that occludes the catalytic site from binding to the substrate in the dark. In response to light, the steric group changes conformation and uncages the catalytic site, allowing access for the substrate.

All LightR-Src structures used for molecular dynamics simulations were created using the Src catalytic domain from PDB: 1Y57 combined with dark and light state VVD from PDB: 2PD7 and 3RH8, respectively. Using UCSF Chimera software <sup>90</sup>, the asymmetric flexible linkers, GPGGSGG and GSGGPG, were respectively added to the N- and C- termini of VVD and the monomers were linked with a long flexible linker of (GGG)<sub>4</sub>G(GGG)<sub>3</sub>. These VVD constructs were then inserted into the active Src catalytic domain using Chimera's structure editor. These flexible linkers were then refined using Modeller <sup>91</sup>. All structures were minimized in NAMD using steepest descent and conjugate gradient <sup>92</sup>. These structures were then equilibrated for 1.5 ns at 37°C with generalized Born implicit solvent with an ion concentration of 0.15 M. All MD simulations were then carried out under these same conditions over 100 ns. Simulations for the LightR constructs were conducted in triplicate for a total simulation time of 300 ns per structure. The RMSD analysis and visualization was carried out using VMD and principal component analysis (PCA) was conducted using the NMWiz GUI for ProDY <sup>93</sup>.

GPGGSGGHTLYAPGGYDIMGYLIQIMNRPNPQVELGPVDTSCALILCDLKQKDTPIV  
YASEAFLYMTGYSNAEVLGRNCRFLQSPDGMVKPKSTRKYVDSNTINTMRKAIDRNAE  
VQVEVVNFKKNGQRNVNFLTMI PV RDETGEYRYSMGFQCETE GSGSGSGSGSGSGGS  
GSGSGSHTLYAPGGYDIMGYLIQIMNRPNPQVELGPVDTSCALILCDLKQKDTPIVYASE  
AFLYMTGYSNAEVLGRNCRFLQSPDGMVKPKSTRKYVDSNTINTMRKAIDRNAEVQVE  
VVNFKKNGQRNVNFLTMI PV RDETGEYRYSMGFQCETEGSGGGPG

Linkers are in grey color. Red and turquoise colors are for the first and second VVD sequences, respectively.

### **C. Molecular Biology**

LightR was codon optimized so that the two tandem VVD DNA sequences are as different as possible to make cloning using PCR easier. LightR sequence was designed so that the two VVD proteins were connected with a flexible linker comprised of twenty-two amino acid sequence of (GGS)<sub>4</sub>G(GGS)<sub>3</sub>. LightR DNA sequence was ordered as a gBlock from Integrated DNA Technologies. The gBlock was amplified using PCR with forward primer encoding a GPGGSGG linker and a 24-28 nucleotide sequence that anneals upstream of the insertion site of interest. The reverse primer encodes a GSGGPG linker and 24-28 nucleotide sequence that anneals downstream of the insertion site of interest. The resulting PCR product of this reaction acts as a megaprimer that we use to insert LightR domain at a site of interest in a gene. Using QuickChange site-directed mutagenesis, we inserted LightR domain into Src gene (bearing Y527F activating mutation) replacing amino acid G288.

We obtained GFP-Abl (gift from Dr. Steve Dudek, UIC) and introduced P242E/P249E mutations to make it constitutively active using site-directed mutagenesis, bRaf V600E was a gift from Dr. John O'Bryan, and iCre from Addgene (#89573), pcDNA3.1\_Floxed-STOP mCherry was a gift from Moritoshi Sato (Addgene plasmid # 122963; <http://n2t.net/addgene:122963>; RRID:Addgene\_122963).

### **D. Antibodies, Chemical Reagents and Cell Lines**

The following antibodies were used: anti-phospho-p130Cas (Y249) (BD Pharmigen cat. no. 558401), anti-p130Cas (BD Pharmigen cat. no. 610271), anti-GFP (Clontech, cat. no. 632381),

anti-paxillin (Fisher Scientific, cat. no. BDB612405), anti-Src (Santa Cruz, cat. no. 8056), anti-GAPDH (Ambion, cat. no. AM4300), anti-phospho-paxillin (Y118) (Invitrogen, cat. no. 44-722G), anti-Myc (Millipore, cat. no. 05-724), anti-phospho-MEK1/2 (Ser17/221) (cell signaling, cat. no. 9121), anti-MEK1/2 (cell signaling, cat. no. 9122), anti-p44/42 (ERK1/2) (cell signaling, cat. no. 9102), anti-p44/42 (ERK1/2) (Thr202/Tyr204) (cell signaling, cat. no. 9101), anti-Src (Santa Cruz, cat. no. 8056), anti-GAPDH (Ambion, cat. no. AM4300).

The following reagents were used: IgG-coupled agarose beads (Millipore, cat. no. IP04-1.5ML), Leupeptin hemisulfate (Gold Biotechnology, cat. no. L-010-5), Aprotinin (Gold Biotechnology, cat. no. A-655-25), Y-27632 dihydrochloride (millipore sigma, cat. no. Y0503), MLCK Inhibitor Peptide 18 (Cayman, cat. no. 224579-74-2). The following cell lines were used: HeLa cells (ATCC, cat. No. CCL- 2), human embryonic kidney HEK293T cells (ATCC, cat. no. CRL-3216), and human embryonic kidney LinXE cell line (derived from HEK 293 cells).

The materials used were: C18 cartridges (Waters, cat. no. WAT02350), TMT11plex (ThermoFisher, cat. no. A34807), TMT10plex (ThermoFisher, cat. no. 90406), Fe-NTA spin columns (ThermoFisher, cat. no. A32992), Trypsin (Promega, cat. no. V5113), Trypsin-digested BSA for coating tubes (Sigma, cat. no. A7906).

#### **E. Expression of Engineered Constructs**

All DNA constructs were overexpressed transiently using Fugene 6 (Promega Corporation) transfection reagent according to the manufacturer protocol.

#### **F. In Vitro Kinase Assay**

A detailed protocol for this experiment was previously described <sup>94</sup>. Briefly, we overexpress in LinXE cells our desired Src kinase constructs, all of which carry a myc tag. We expose the

cells to continuous blue light (3 mW/cm<sup>2</sup>, 465 nm wavelength) for the indicated times or keep them in the dark, then collect cell lysate in the dark using the lysis buffer (20 mM HEPES-KOH, pH 7.8, 50 mM KCl, 100 mM NaCl, 1 mM EGTA, 1% NP40, 1 mM NaF, 0.1 mM Na<sub>3</sub>VO<sub>4</sub>, aprotinin 16 µg/ml, and Leupeptin hemisulfate 3.2 µg/mL). We then centrifuge the lysate at 4,000 rpm, 4°C, for 10 minutes, and incubate the cleared lysate with the beads conjugated with the anti-myc antibody (4A6 from Millipore-Sigma) for 1.5 hours at 4°C. Beads were then washed with wash buffer (20 mM Hepes-KOH, pH 7.8, 100 mM NaCl, 50 mM KCl, 1nM EGTA, 1% NP40) and then with kinase reaction buffer (25 mM HEPES, pH 7.5, 5 M MgCl<sub>2</sub>, 0.5 mM EGTA, 0.005% BRIJ-35). The beads were then incubated with 0.1 mM ATP and ~0.05 mg/ml paxillin in kinase buffer (25 mM HEPES pH 7.5, 5 mM MgCl<sub>2</sub>, 0.5 mM EGTA, 0.005% BRIJ-35) in 37°C for 10 minutes. The reaction is terminated by resuspending the reaction in 2X Laemmli sample buffer and 2-Mercaptoethanol (20:1 ratio) then boiling it for 5 minutes. The phosphorylation of paxillin at Y118 residue was examined by western blotting.

#### **G. Biochemical Characterization of LightR Kinases**

LinXE cells grown in 3 cm plates were transfected overnight with LightR construct of interest and kept in dark the entire time. Next day, the cells were exposed to light by placing them at 10 cm above an HQRP® LED Plant Grow Panel Lamp System (3 mW/cm<sup>2</sup>, 465 nm wavelength). Temperature was maintained during incubation times by placing the setup inside a tissue culture incubator. Light was shining continuously for the desired time. In experiments that required cycles of activation and inactivation, we simply unplugged the LED panel during inactivation times and plugged it back in during activation times before we lysed the cells. At the end of the experiment time course, cells were immediately collected in the dark using safe red-lights with 700 µl of 2X Laemmli sample buffer and 2-Mercaptoethanol (20:1 ratio) and boiled

for 5 minutes. 10-15 ul of the cell lysates were analyzed by a western blot to probe for the phosphorylation of endogenous proteins.

## **H. Characterization of LightR-Cre**

To assess LightR-Cre activity we used the previously described Floxed-STOP-mCherry reporter system <sup>65</sup>. LinXE cells were co-transfected overnight with LightR-Cre-iRFP670 and Floxed-STOP-mCherry DNA constructs (1:9 ratio) and kept in the dark. Next day cells were pulsed with light using the HQR® LED Plant Grow Panel Lamp System (3 mW/cm<sup>2</sup>, 465 nm wavelength). A microcontroller (Arduino Uno) and power relay (IoT Relay, Digital Data Loggers INC.) were used to turn on the LED panel for 2 seconds every 10 seconds. Cells were then imaged using EVOS™ Auto 2 Invitrogen fluorescence microscope to analyze the expression of mCherry reporter.

## **I. Production of LightR-Src HeLa Stable Cell Line**

LightR-Src was subcloned into a lentiviral plasmid with restriction enzyme digest and ligation method, then lentivirus was produced and used to transduce HeLa cells. Briefly, the LightR-Src-mCherry gene was PCR-amplified with primers that introduced restriction sites NotI and BsiWI on the 5' and 3' end, respectively. This PCR product and LeGO-iV2 from Addgene (#27344) were digested with NotI and BsrGI and then ligated to generate a LightR-Src-mCherry lentiviral construct. This construct was then co-transfected with pMD2.G (Addgene #12259), a VSV-G lentivirus envelope expressing plasmid, and psPAX2 (Addgene #12260), a 2nd generation lentiviral packaging plasmid, into HEK 293T cells (ATCC CRL-3216). After 1-3 days, virus containing supernatant was used to directly infect HeLa cells. Transduced HeLa cells were sorted via FACS by selecting the brightest 20 percentile of mCherry expressing cells.

## **J. Mass Spectrometry**

### **1. Sample Preparation.**

Urea lysates were prepared as previously described<sup>95</sup>. Briefly, lysate was reduced with 10 mM dithiothreitol (DTT), alkylated with 55 mM iodoacetamide, and digested with trypsin overnight. Digested peptides were subjected to desalting using C18 cartridges (Waters), and lyophilized. Peptides were labeled with TMT 11plex isobaric mass tags and stored at -80 C.

### **2. Phosphotyrosine Enrichment and Mass Spectrometry Analysis.**

TMT-labeled peptide samples were subjected to a previously described two-step enrichment process<sup>95</sup>, with the following modifications: First, 12 µg of “super” 4G10<sup>96</sup> was utilized in place of the commercial antibody from Millipore Sigma. Second, peptides were eluted from antibody-conjugated beads twice with 0.2% trifluoroacetic acid in milliQ water. Eluted peptides were directly added to immobilized metal affinity chromatography (IMAC) Fe-NTA spin columns (ThermoFisher Scientific). Fe-NTA columns were used according to the manufacturer’s instructions. Phosphopeptides were eluted twice with 20 µL of elution buffer into a BSA-coated 1.5 mL tube, and eluted peptides were dried down in a speed vacuum concentrator. Dried peptides were resuspended in 10 µL of 5% acetonitrile in 0.1% formic acid and loaded directly onto an in-house packed analytical capillary column (50 µm ID × 12 cm, 5 µm C18) with an integrated electrospray tip (1–2 µm orifice). Eluates were then subjected to LC-MS/MS as previously described with the following modifications<sup>95</sup>:

1) The mass spectrometer was operated with a spray voltage of 2.5 kV. 2) Selected ions were HCD fragmented at normalized collision energy 32%. 3) MS/MS acquisition was performed at a resolution of 60,000. Limited LC-MS/MS analysis of the most abundant peptides

to adjust for channel-to-channel loading variation was carried out on an Orbitrap Q-Exactive Plus mass spectrometer using ~15 ng of peptide. Supernatant was loaded onto an acidified trapping column and analyzed with gradients as follows: 0–13% solvent B in 4 min, 13–42% in 46 min, 42–60% in 7 min, 60–100% in 3 min, and 100% for 8 min, before equilibrating back to Solvent A. Full scans (MS1) were acquired in the  $m/z$  range of 350–2,000 at a resolution of 70,000 ( $m/z$  100). The top 10 most intense precursor ions were selected and isolated with an isolation width of 0.4  $m/z$ . Selected ions were HCD fragmented at normalized collision energy (NCE) 33% at a resolution of 70,000.

*Peptide identification and quantification.* Raw mass spectral data files were processed as previously described<sup>95</sup> with the following changes: 1) Raw files were processed with Proteome Discoverer version 2.2.0.388 (ThermoFisher Scientific) and searched against the human SwissProt database using Mascot version 2.4.1 (Matrix Science). 2) Peptide spectrum matches (PSMs) for phosphopeptides were filtered for ion score  $\geq 20$  and precursor isolation interference ( $< 35\%$ ), and PSMs for the most abundant peptides in IP supernatant runs were filtered for ion score  $\geq 25$ .

*Data Analysis.* Data from three independent mass spectrometry runs was transformed as previously described using IP supernatants run on the Q-Exactive Plus<sup>95</sup>. For each phosphopeptide, relative quantification was represented as a ratio between TMT ion intensities from each time point (10 s, 30 s, 1 min, 5 min, 60 min) and the 0 second LightR-Src condition. Data were filtered for peptides that were common to each of three runs.

*Visualization and Statistical Analysis.* To identify phosphopeptides with significant changes in abundance relative to the 0 s LightR-Src condition, we utilized paired Student's t-test ( $p$ -value  $< 0.05$ ). Additionally, to ensure phosphopeptide changes were not simply background, we filtered



for peptides with average abundances ( $n=3$ ) that were  $>1.4$  relative to the 0 second LightR-Src condition. The average abundance for each phosphopeptide was log2-transformed and visualized using MATLAB (version R2019b, Bioinformatics Toolbox version 4.13, MathWorks). Data were plotted with the 'clustergram' function with hierarchical clustering using Euclidean distance.

*PCA and STRING network analysis.* For PCA, all phosphoproteomic data were normalized to basal abundances in LightR-Src cells (0s LightR-Src HeLa). Phosphopeptide abundances were averaged across all three biological replicates, then log2-transformed. Abundances were re-centered around 0 by subtracting the mean of each phosphopeptide across all conditions. PCA was performed using Scikit-learn (v0.19.1) in Python (v3.6.0). For STRING network analysis of principal component 1, loading scores from PCA were extracted for all phosphopeptides, rank-ordered (decreasing), and the gene IDs of all phosphopeptides with loading score  $> 0.05$  were provided as input to STRING (v11.0) <sup>97</sup>. Disconnected nodes were hidden from the network representation.

*Data availability.* The raw mass spectrometry data and associated tables have been deposited to the ProteomeXchange Consortium via the PRIDE partner repository with the dataset identifier: PXD018162.

Username: reviewer90800@ebi.ac.uk

Password: g63C5lYd

## **K. Cell imaging and image analysis**

### **1. Sample Preparation and Imaging Hardware**

On the day of imaging, cells were seeded 3 hours before imaging at 30-40 % confluency on a glass coverslip that was coated overnight with fibronectin (5 mg/L). In experiments using inhibitors, cells were pretreated with the appropriate inhibitor 2 hours before imaging experiments. Live cell imaging was performed after 2-4 hours from seeding HeLa cells on coverslips and transferred to Leibovitz (L-15) imaging medium with 5% fetal bovine serum. Cells were kept at 37 C using an open heated chamber (Warner Instruments). Cells were imaged using an Olympus IX-83 microscope controlled with Metamorph software and equipped with Xcite 120 LED (Lumen Dynamics), objective-based total internal reflection fluorescence (TIRF) system, Olympus UPlanSAPO 40× (oil, N.A. 1.25) objective, PlanApo N 60× TIRF microscope objective (oil, NA 1.45), 445-nm and 561-nm laser lines, Xcite 120 LED (Lumen Dynamics) light source, and Image EMX2 CCD (Hamamatsu) camera.

### **2. Cell Spreading and Protrusive Activity Analysis**

We transiently overexpressed stargazin-iRFP to uniformly label the plasma membrane. Using epifluorescence imaging, we selected cells co-expressing LightR-Src-mCherry and stargazin-iRFP. Time-lapse images were acquired every minute. To induce cell spreading, cells were globally pulsed with 50 ms of blue light every second, 50 pulses every minute. Stargazin-iRFP images were used to create a binary mask based on intensity thresholding. The binary mask was generated by MovThresh script using Matlab software <sup>98</sup>. Then using Metamorph, we calculated cell area. To measure the change in area for each cell, we divided the cell area at any

given time by the average area of the same cell prior to blue light irradiation. Finally, for cell area and protrusive activity change, the average and 90% confidence interval were calculated for each time point of all cells treated in similar conditions.

### 3. **Local blue light stimulation**

A focused beam of 445 nm laser light was delivered to local area at the cell periphery. The light was fixed throughout the stimulation period and was irradiated for fifty-four seconds every minute.

### 4. **Polarity index calculation**

Polarity index calculation was adopted from a previously described method<sup>14</sup>. Briefly, we used Metamorph software to calculate the angle of deviation ( $\theta$ ) of the cell's centroid from the blue light in response to local blue light stimulation (Figure 9). To obtain the polarity index, we calculated  $\cos \theta$ .

### 5. **Centroid shift**

The centroid shift distance (Figure 9) was determined using Metamorph by measuring the number of pixels the centroid moved in response to local blue light and multiplying this value by the pixel size (0.4  $\mu\text{m}$  for a 40X objective) on our camera. Centroid shift ( $\mu\text{m}$ ) = number of pixels x 0.4.

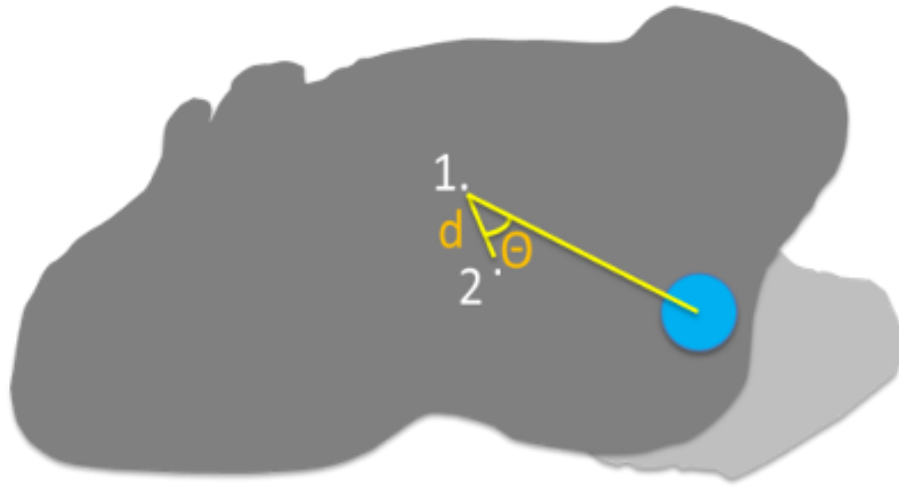


**Figure 9: Polarity index and centroid shift.** A diagram showing the centroid shift distance ( $d$ ) traveled by the centroid of the cell between the onset of local blue light stimulation (1) and the end of stimulation (2). The angle of deviation ( $\theta$ ) represents the extent of divergence of the cell's centroid movement direction from the location of blue light. Light grey represents the area protruded by the cell in response to local LightR-Src stimulation.

## 6. Quantification of Cell Edge Dynamics

In order to quantify the response of cell edge to the local kinase activation with the light, we performed the following steps of the analysis:

*Cell edge extraction.* Each cell in the time-lapse records was segmented to obtain the binary cell mask at every time frame. The standard pixel wise tracing of an object boundary was applied to extract the cell outline. Then, the outlines were processed with the CellGeo software package<sup>98</sup> to smooth the edge by removing all fine-scale (slender) protrusions like filopodia and retraction fibers. In addition, the boundaries were resampled with a large number of points ( $N = 700$ ) to achieve the consistency of the boundary representations between different cells and different time points.

*Velocity calculation.* The velocity of each point representing the cell edge at time  $t$  was calculated as the distance to the nearest point of the cell edge at time  $t + \Delta t$  divided by  $\Delta t$ . In this study, we used  $\Delta t = 5$  minutes.

*Velocity kymographs.* In order to represent the cell edge dynamics over the recording time as a single graph, we constricted kymographs by stacking the velocity values along the cell edge sequentially from the first (top) to the last (bottom) time frame. The resulting data matrix was visualized as a color map with the highest positive velocity (protrusion) in red and the highest negative velocity (retraction) in blue. Although we use the same number of points in the cell

boundary representation, the perimeter of these boundaries varies from frame to frame, which can create artificial horizontal misalignment depending on how the first point of the boundary is chosen. To avoid this issue at the edge region of our interest, we used our automated algorithm (see below) to align velocity values such that the edge position along the line of the most active protrusion near the site of the light activation was in the middle of the kymograph. This way, any boundary misalignments due to the variation of the cell perimeter can occur only on the sides of the kymographs, where our further comparative quantification was not performed.

*Alignment of kymograph rows.* Most of the processing steps of the kymograph construction algorithm was adopted from the EdgeProps software <sup>99</sup>. The only difference is the method of finding the point on the cell outline at each time frame to be positioned in the middle column of the kymograph. In this method, we first apply Gaussian Filter to the cell outline to obtain a smoothed representation of the cell edge at times  $t$  and  $t + \Delta t$ . Then, we measure the distance from each point on the boundary at time  $t$  to the boundary at time  $t + \Delta t$  along the directions of the normal vectors to the boundary at time  $t$ . The local maximum of this measure in the vicinity of the laser activation is taken as the middle position in the velocity kymograph. The calculation of this local maximum is repeated by the algorithm for each time frame so that all boundaries are consistently aligned over the whole-time record.

*Comparative analysis of the light-induced edge movement.* Once the edge velocity from different time frames is properly centered in the kymographs, we can compare the response of different cell types by averaging the kymographs of all cells in a given phenotypic group. Furthermore, by

choosing a central stripe in the kymographs (the area between the vertical dash lines in figures 23a-c) and averaging it along the perimeter, we convert the spatiotemporal representation of the protrusive cell response at the vicinity of the stimulation site into the velocity versus time plots shown in figure 23d-f. In this study, we use the stripe width of 42 pixels, which corresponds to arc length of 11.2  $\mu\text{m}$ .

*Statistical analysis of the light-induced edge movement.* After converting the spatiotemporal response of the cell edge to the light activation into the velocity versus time plots as described above, we identified the average velocity value for each cell. To evaluate statistical significance of the difference in these measures between cell phenotypes, we used Wilcoxon test, the nonparametric equivalent of the two sample t-test.

## IV. RESULTS

### A. Design of LightR Domain

To modulate protein activity with light, we engineered a Light-Regulated (LightR) domain that can potentially function as an allosteric switch when inserted into a catalytic domain of an enzyme. LightR comprises two tandemly connected Vivid (VVD) photoreceptor domains from *Neurospora crassa*<sup>100-103</sup>. VVD is a monomer in the dark and forms an antiparallel homodimer upon illumination with blue light<sup>100-103</sup>. Dimerization is accompanied by a major flip of the N-terminal tail bringing it close to the C-terminus of another VVD in the dimer (Figure 10a)<sup>101-103</sup>. We, therefore, envisioned that a tandem connection of two VVDs via a flexible linker would generate a clamp-like switch of 335 amino acid total size that opens in the dark and closes in response to blue light. We hypothesized that inserting this LightR clamp domain into a small loop between two structured regions within the catalytic domain will enable light-mediated regulation of the protein activity. In the dark, the opened LightR clamp should distort the native structure of the catalytic domain and thereby inactivate the protein. Illumination with blue light will close the clamp, bringing the N- and C-termini of LightR together and by that recovering the native structure of the catalytic domain resulting in the restoration of the protein activity (Figure 10b).



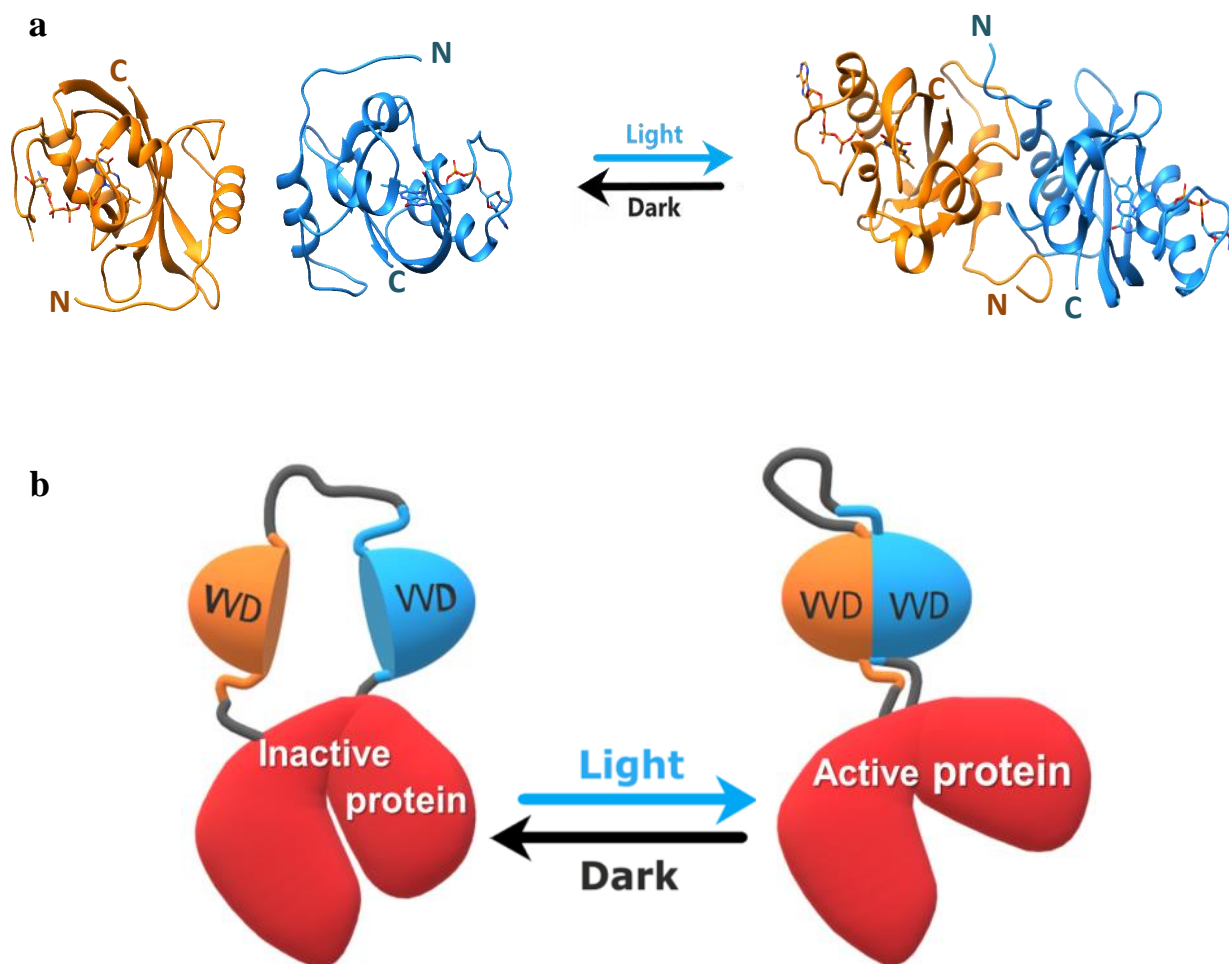


**Figure 10: VVD photoreceptor and LightR design.** **a**, Crystal structures of two Vivid monomers in the dark state (PDB: 2PD7), and VVD dimer in the lit state (PDB: 3RH8). **b**, Cartoon representation of LightR design. Two VVD photoreceptors inserted in the catalytic domain disrupts the catalytic activity of the protein in the dark. Dimerization of VVD in response to blue light restores the protein activity.

## **B. Molecular Dynamic Studies Suggests LightR is an Allosteric Switch**

As an initial model, we chose to generate light-regulated tyrosine kinase Src (LightR-Src). Our previous studies demonstrate that position Gly288 in Src catalytic domain can be employed as an insertion site for LightR domain to achieve allosteric control of activity (Figure 11a) <sup>16</sup>. We first performed molecular dynamics simulations of the designed LightR-Src catalytic domain to predict a possible mechanism for regulation of kinase activity by LightR domain. The structures were modeled using existent crystal structures of c-Src catalytic domain and modified crystal structures of VVD in the lit and dark state with a 22-residue flexible linker of (GGS)<sub>4</sub>G(GGS)<sub>3</sub> between the two VVDs, and flexible GPGGSGG and GSGGPG linkers between VVD and Src. Analysis of LightR-Src in the dark shows increased root mean square deviation (RMSD) of the catalytic domain compared to the active wild type Src (Figure 11a-c), and strong correlation between the motion of the residues in LightR clamp and in Src catalytic domain (Figure 12), suggesting an allosteric mechanism. In contrast, the lit state of LightR-Src exhibits much lower RMSD, closer to wild type Src (Figure 11a-c) and loses the motion correlation between LightR domain and Src residues (Figure 12). This indicates that the open conformation of LightR clamp in the dark can cause changes in the catalytic domain of Src that will be reversed upon illumination with blue light. Interestingly, LightR-Src in the dark shows substantial deviation of the G-loop, a critical functional element of most protein kinases <sup>104, 105</sup> (Figure 11a-c and Figure 12). This suggests an allosteric mechanism whereby LightR domain regulates kinase activity via disruption of the G-loop.

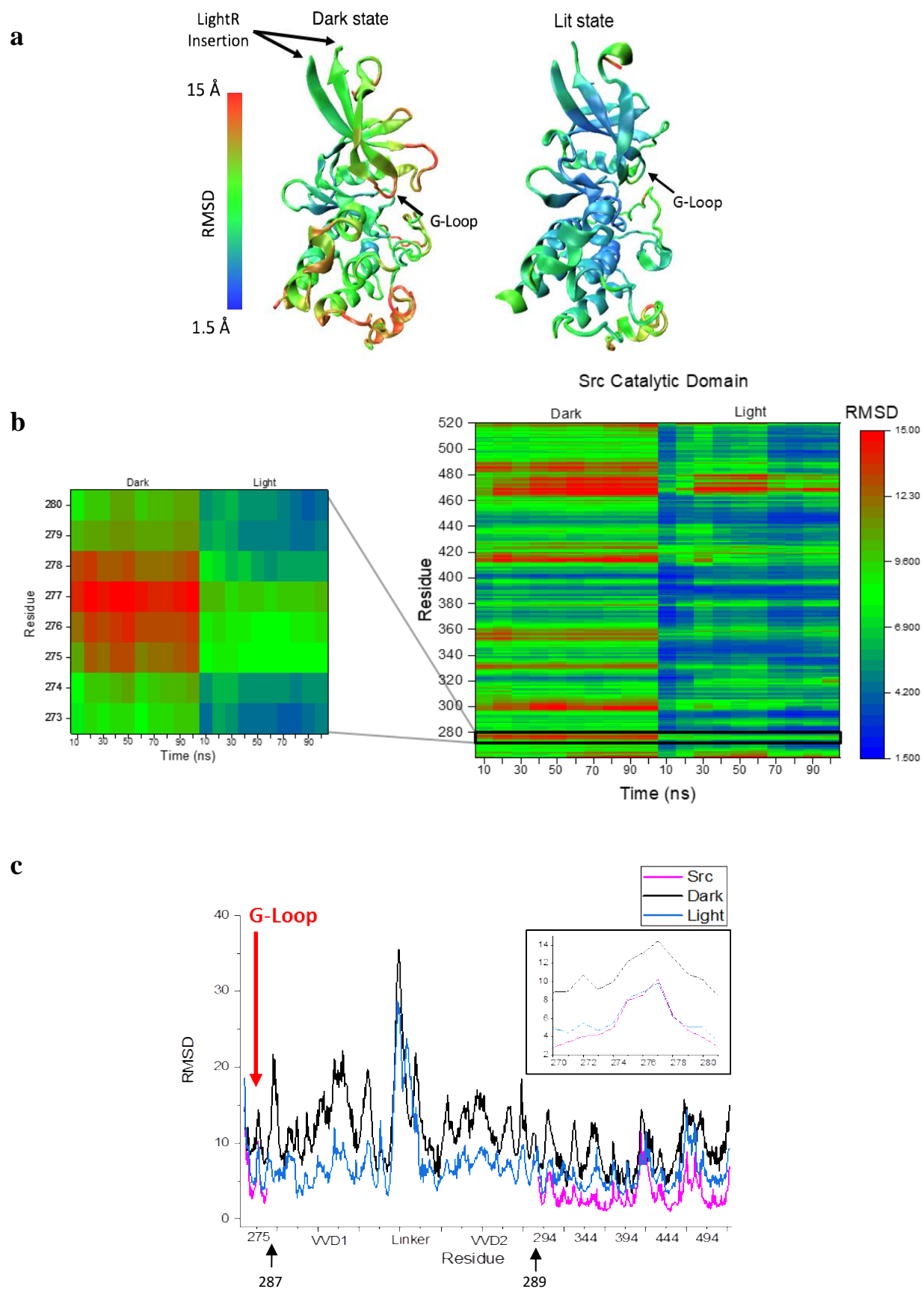


**Figure 11: LightR-Src molecular dynamics.** **a**, Computational modeling of structural changes in the catalytic domain of LightR-Src. Color scale reflects the degree of deviation from the position in the crystal structure of Src (PDB: 1Y57). **b**, Comparative heat map of RMSD for each residue over the course of the simulation for Src catalytic domain in lit and dark states. Zoomed in insert shows changes in the G-loop. **c**, Comparison of average RMSD of all catalytic domain residues in the lit and dark state of LightR-Src, as well as the wild type active Src. All figures represent an average of three simulations ran for a duration of 100 ns each. Arrows point at Src residues that directly flank LightR domain.

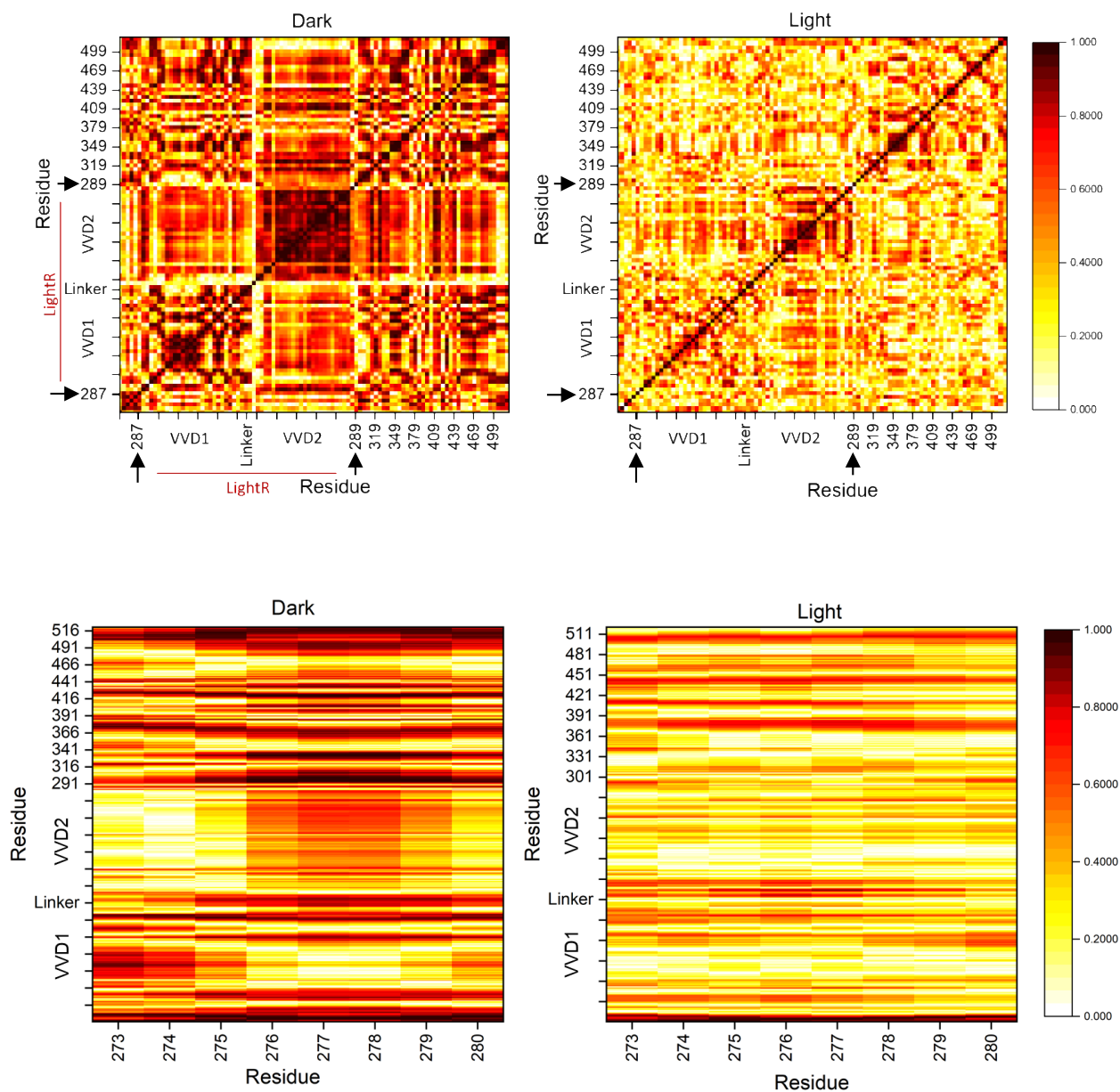


**Figure 12: Cross correlation maps of the dark and lit states of LightR-Src.** Residues with uncorrelated motion have a correlation of 0 while perfectly correlated motion has a value of 1. Lower heat maps represent the correlation between the G-loop residues (x-axis) and all other residues within LightR-Src catalytic domain (y-axis) in the dark and lit states.

### C. Blue Light Activates LightR-Src

LightR-Src construct bears a Y527F mutation (avian cSrc position) and is fused with mCherry and myc tag at the C-terminus. Y527F mutation disrupts its autoinhibition and prevents the negative regulation of Src by endogenous mechanisms<sup>16, 106</sup>. We employed this to ensure that LightR-Src is only regulated by light. To test if LightR insertion regulates Src kinase function with light, we performed an *in-vitro* kinase assay of LightR-Src immuno-precipitated from LinXE cells and incubated with its substrate paxillin. We compared it to the activity of the kinase dead LightR-Src (D388R) and the constitutively active Src (Y527F). Our results show that LightR insertion in Src completely disrupts its function in the dark and recovers it in response to blue light to levels comparable to that of constitutively active Src, as judged by the level of phospho-paxillin (Y118) (Figure 13a).

To test the regulation of LightR-Src in living cells, we evaluated changes in the phosphorylation of known Src substrates, p130Cas (Y249) and paxillin (Y118)<sup>107, 108</sup>. Our results show that illumination of LinXE cells transiently expressing LightR-Src induces robust phosphorylation of endogenous paxillin and p130Cas (Figure 13b). Importantly, the catalytically inactive mutant of LightR-Src (D388R) that was exposed to blue light did not show any increase in phosphorylation of Src substrate (Figure 13b). This demonstrates that the increase in phosphorylation is a direct consequence of LightR-Src activation and that blue light by itself had no effects on the Src targets. Activation time-course demonstrates noticeable phosphorylation of Src targets after only two minutes of light irradiation (Figure 13c). The level of activity of LightR-Src can be regulated by the attenuation of light intensity (Figure 13d). These data support our model for the regulation of kinase activity using LightR clamp domain and demonstrate efficient and specific regulation of LightR-Src in living cells.

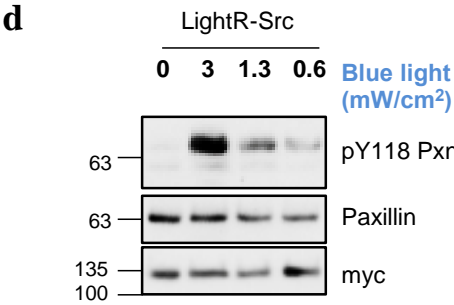
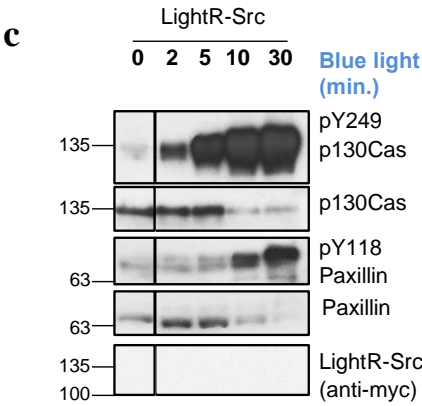
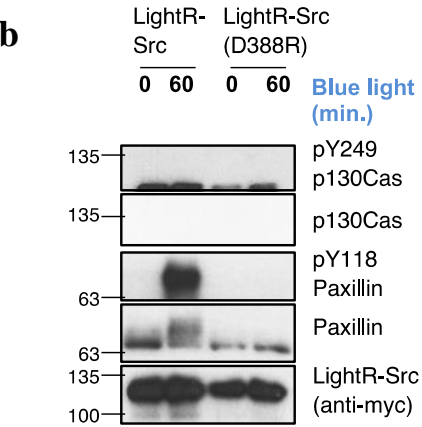
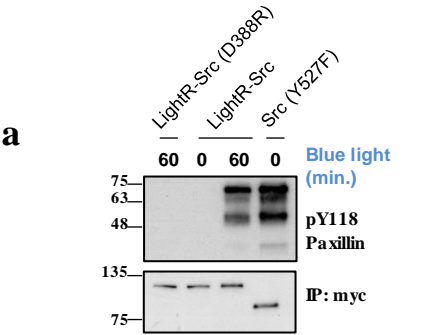
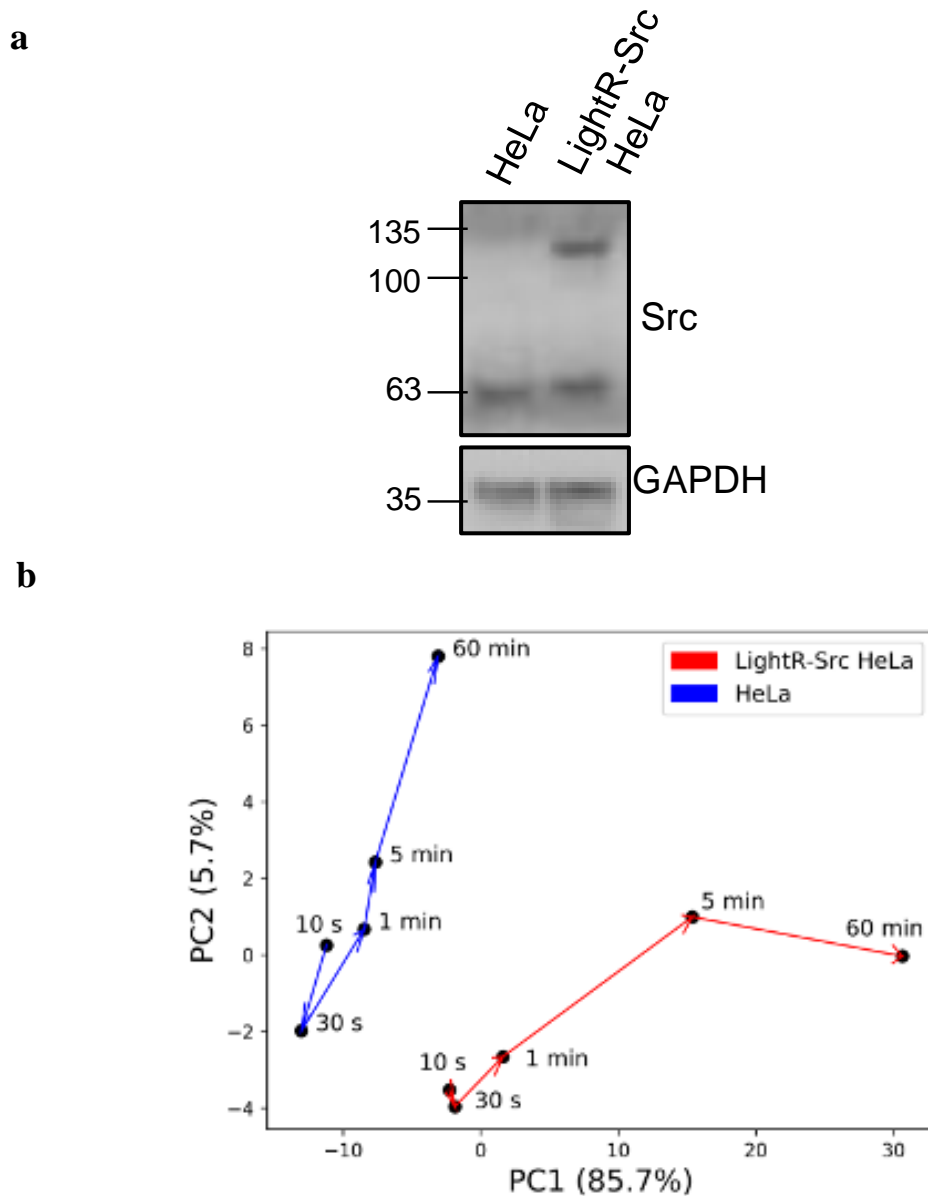


**Figure 13: Characterization of LightR-Src.** **a**, In vitro kinase assay of immunoprecipitated Src constructs. LinXE cells transiently expressing the indicated Src constructs bearing mCherry and myc tag. Cells were exposed to continuous blue light for 1 h and immediately immunoprecipitated. Purified paxillin was used as a substrate. **b**, **c**, LinXE cells expressing the indicated LightR-Src construct were illuminated with blue light for the specified periods of time. Cell lysates were probed for phosphorylation of Src substrates, paxillin and p130Cas. **d**, LinXE cells expressing LightR-Src were exposed to different blue light intensities for fifteen minutes. Cell lysates were probed for phosphorylation of endogenous paxillin on Y118. All experiments were repeated at least 3 times with similar results.



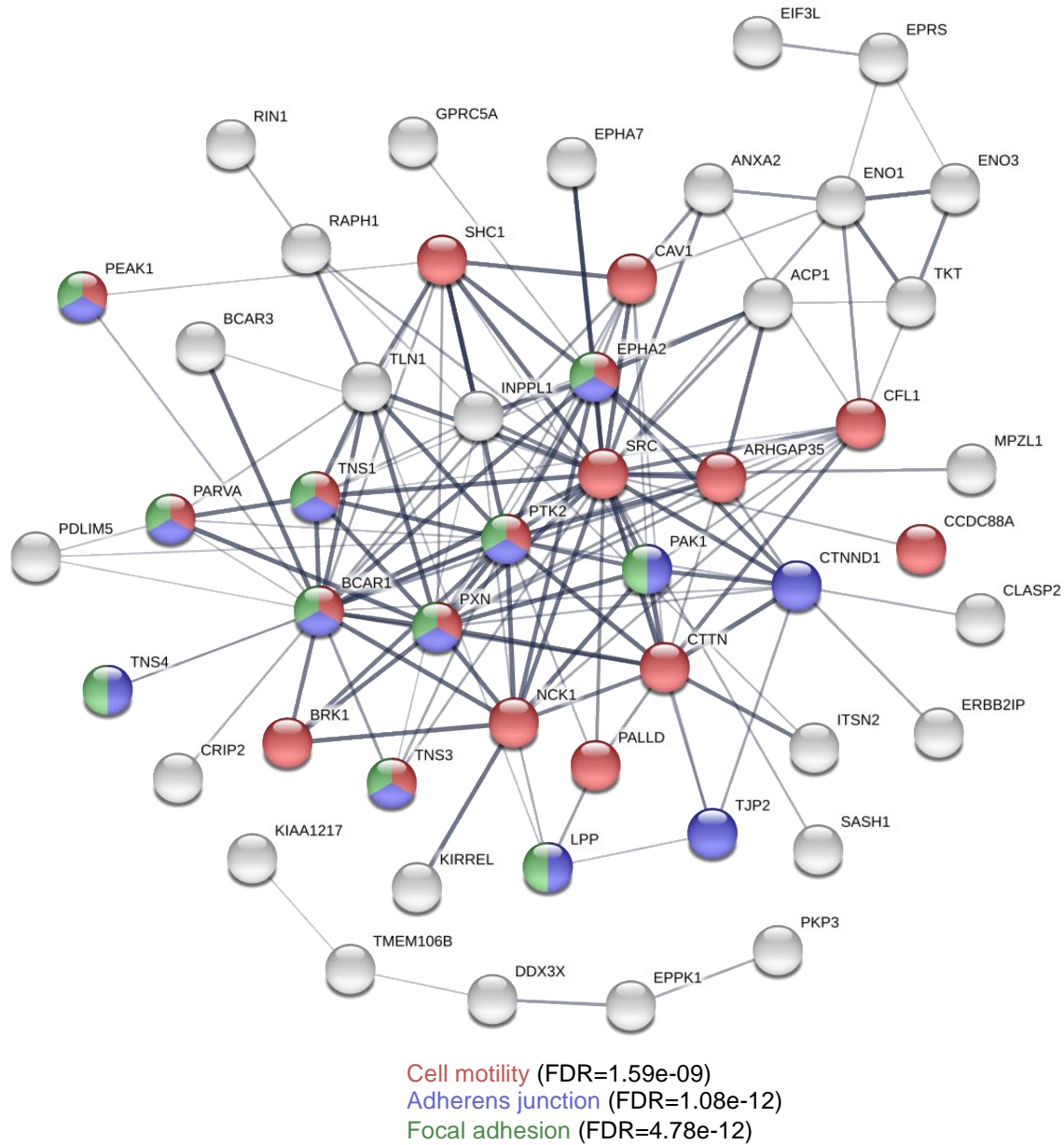
**D. Cells expressing LightR-Src Undergo Broad Phosphorylation Events Upon Light Illumination.**

One central advantage of a light-regulated enzyme activity is the opportunity for its tight temporal control. We generated LightR-HeLa cells, a stable cell line that expresses LightR-Src-mCherry-myc in HeLa cells at levels comparable to that of endogenous Src (Figure 14a). We sought to evaluate the phosphorylation of a broad panel of Src substrates using quantitative LC-MS/MS analysis. Principal component analysis (PCA) revealed that LightR-Src-expressing cells exhibited broadly distinct phosphoproteome dynamics from cells that do not express LightR-Src following light exposure (Figure 14b).



**Figure 14: Principal component analysis.** **a**, Total cell lysate collected from HeLa and LightR-Src HeLa and probed with Src antibody. Higher band represents LightR-Src-mCherry-myc protein and lower band represents endogenous Src. **b**, Principal component analysis (PCA) of phosphoproteomic responses to different time of light exposure in HeLa cells with and without LightR-Src construct.

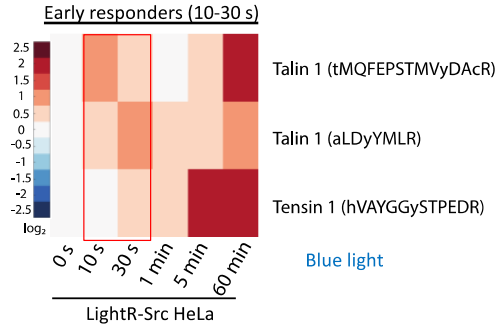
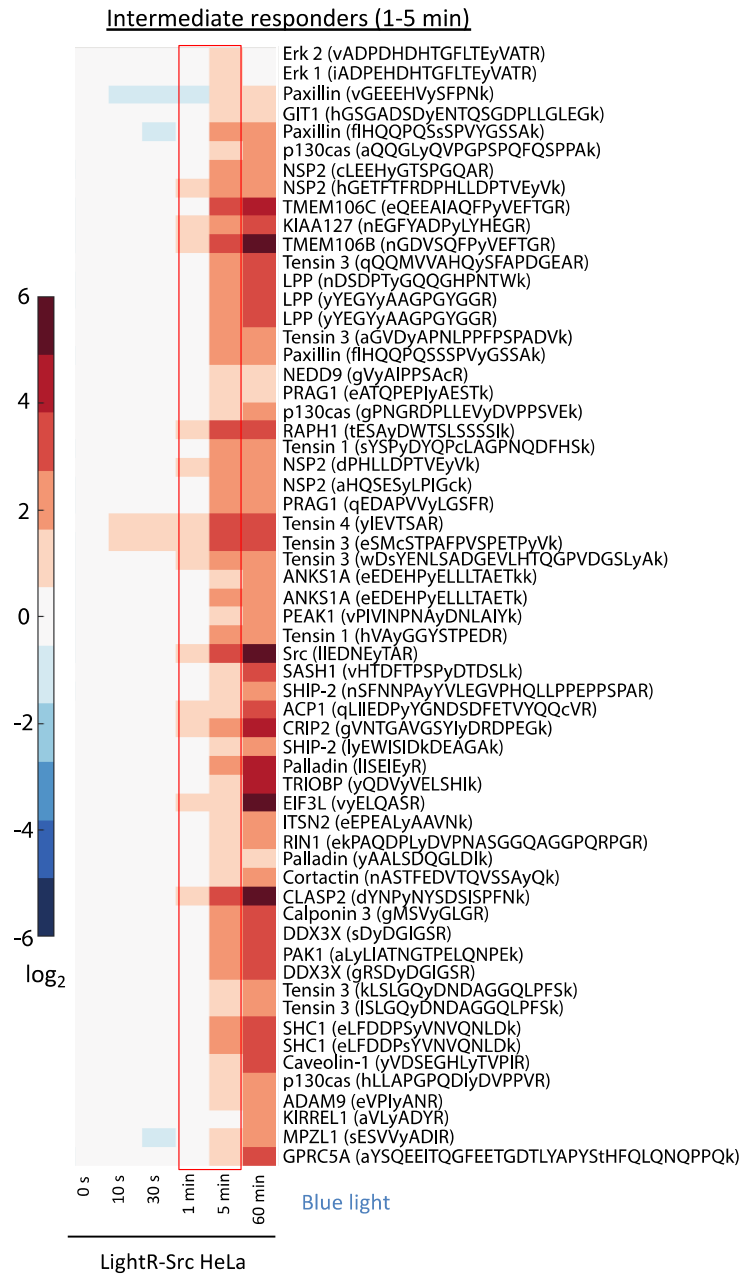
Protein interaction network analysis along with principal component 1 revealed that LightR-Src-induced phosphorylation events were enriched for cell migration, cell adherens junctions, and focal adhesions, processes known to be driven by Src activation (Figure 15).



**Figure 15: STRING biological network analysis.** STRING analysis on phosphopeptides with high weight in principal component 1 (PC1), colored by several highly enriched biological processes related to cell motility and adhesion.

### **E. LightR-Src Reveals Downstream Phosphorylation Temporal Dynamics**

Phosphorylation of known Src targets including caveolin1 (Y14), p130Cas (Y12, Y128, Y249, and Y287), paxillin (Y88 and Y118), p120 catenin (Y217 and Y228), and cortactin (Y421) was significantly increased in LightR-Src HeLa cells, but not in control cells, exposed to blue light. Regulation of Src by light provides tight temporal control of its activity. Therefore, to assess the temporal dynamics downstream of LightR-Src signaling, we analyzed changes in the phosphoproteome at different time points after LightR-Src activation. Several distinct phosphorylation kinetics profiles were identified. “Early responders” exhibited a significant increase in phosphorylation as early as ten and thirty seconds after LightR-Src activation, further demonstrating fast activation of LightR-Src (Figure 16a). “Intermediate responders” show increased phosphorylation at 1 and 5-minute time points (Figure 16b). Interestingly, we detect Src autophosphorylation on Y416 at 1 minute (Figure 16b), indicating that Src phosphorylates some targets before it even undergoes autophosphorylation. A group of “late responders” was phosphorylated at 1 hour (Figure 16c). A distinct group of proteins comprised of MAP kinases ERK1 and ERK2 exhibited only transient increase in phosphorylation at 5 minutes (Figure 16b, top two rows). This phosphorylation is mediated by upstream MAP kinase cascades and leads to activation of ERK kinases<sup>2, 18, 109</sup>. Thus, our data indicate that Src only transiently activates specific MAP kinase pathways. Importantly, all these phosphorylation changes were not detected in control HeLa cells without LightR-Src exposed to blue light. Overall, these results demonstrate that LightR-Src is able to phosphorylate known Src substrates, show fast kinetics of LightR-Src signaling and uncover distinct temporal effects of Src activation on protein phosphorylation in living cells.

**a****b**

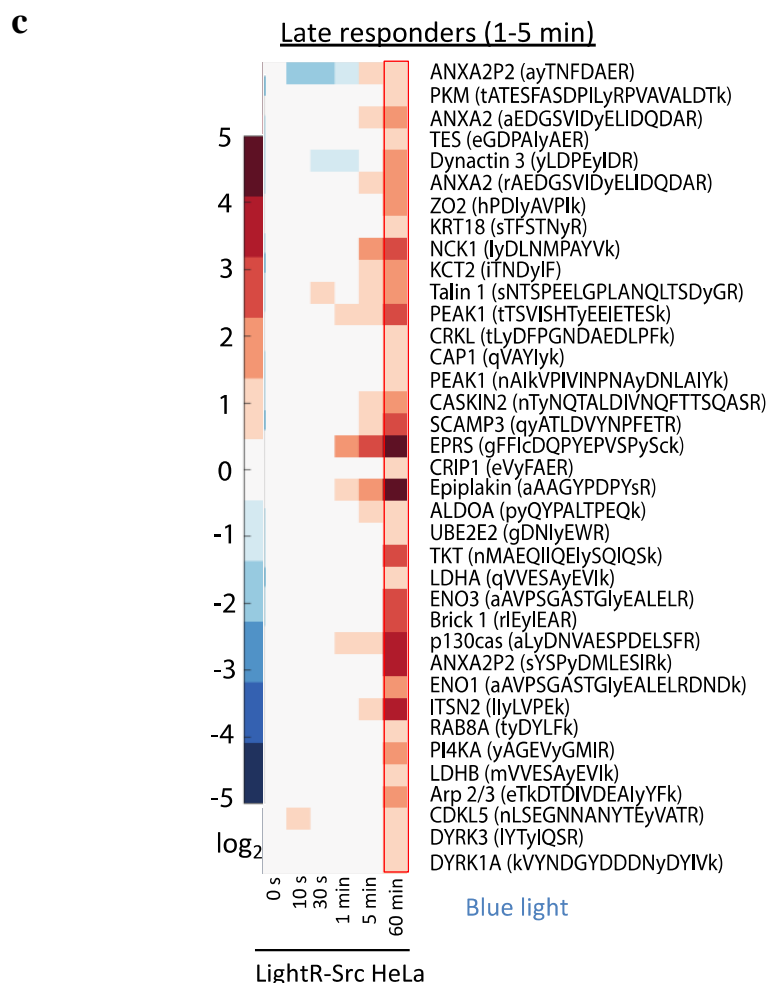


**Figure 16: Temporal changes in protein phosphorylation induced by LightR-Src activation.** Heatmaps represent three categories defined by the initial time of upregulation: **a**, Early responders (10-30 sec); **b**, Intermediate responders (1-5 min); and **c**, Late responders (1 hour). Phosphopeptides are clustered using the correlation distance metric. Columns represent relative abundances of a phosphopeptide at given timepoints normalized to 0 seconds. Data shows average of three independent experiments.

## **F. LightR-Src Activation is Reversible**

Since VVD dimerization is reversible<sup>9</sup>, we hypothesized that LightR-Src should become inactive when light is switched off. Indeed, incubation of cells in the dark following illumination led to a significant decrease in phosphorylation of paxillin (Figure 17a). However, it took up to 2 hours for the phosphorylation to return to basal levels, indicating slow inactivation kinetics of LightR-Src (Figure 17a). To achieve faster inactivation of LightR-Src, we introduced I85V mutation into both VVD domains. This mutation reduces the half-life of VVD dimer in the dark from 18,000 seconds to 780 seconds and thus should facilitate faster LightR-Src inactivation<sup>110</sup>. Indeed, our results revealed that compared to the original LightR-Src, I85V/I85V variant (FastLightR-Src) demonstrated much faster reversibility. Within two minutes after the light was switched off, we observed a significant decrease in paxillin phosphorylation (Figure 17b). By fifteen minutes, phosphorylation reached basal levels (Figure 17b). Thus, modifications of the VVD domains allowed us to tune the off-kinetics of the LightR switch. However, since I85V mutation results in faster cycling of VVD from the lit to the dark state, FastLightR-Src reaches around half the activity of LightR-Src for the same activation time (Figure 17c).



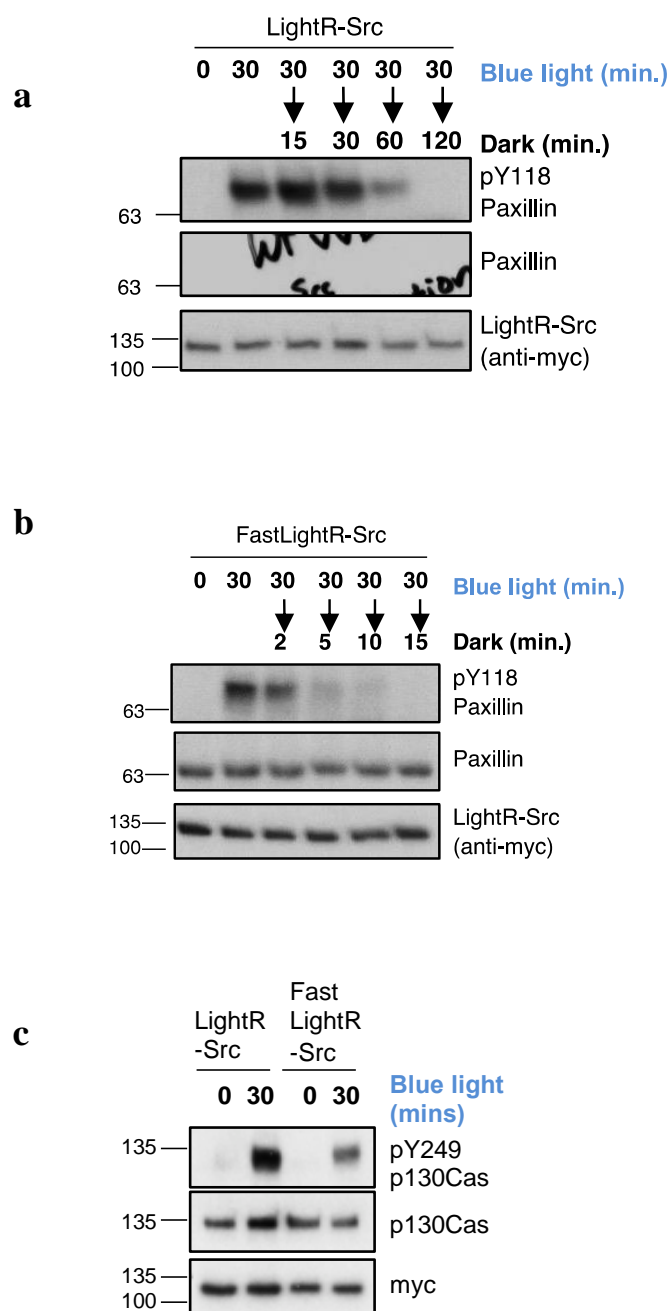


**Figure 17: Reversibility of LightR- and FastLightR-Src.** a-c, LinXE cells transiently expressing the indicated constructs were exposed to blue light for specified times and then either placed in the dark for different times. All experiments were repeated at least 3 times with similar results.

Protein kinases are often activated transiently and can undergo repeated cycles of activation/inactivation<sup>28, 111-114</sup>. These oscillations of kinase activity can drive a specific biological response<sup>28, 111-113</sup>. Thus, we wanted to determine whether FastLightR construct can be used to mimic oscillations of kinase activity in living cells. To test this, FastLightR-Src was activated for two periods of twenty minutes each, separated by ten minutes of deactivation. Our results reveal successful cycles of activation and inactivation as indicated by changes in phosphorylation of p130Cas (Figure 18).

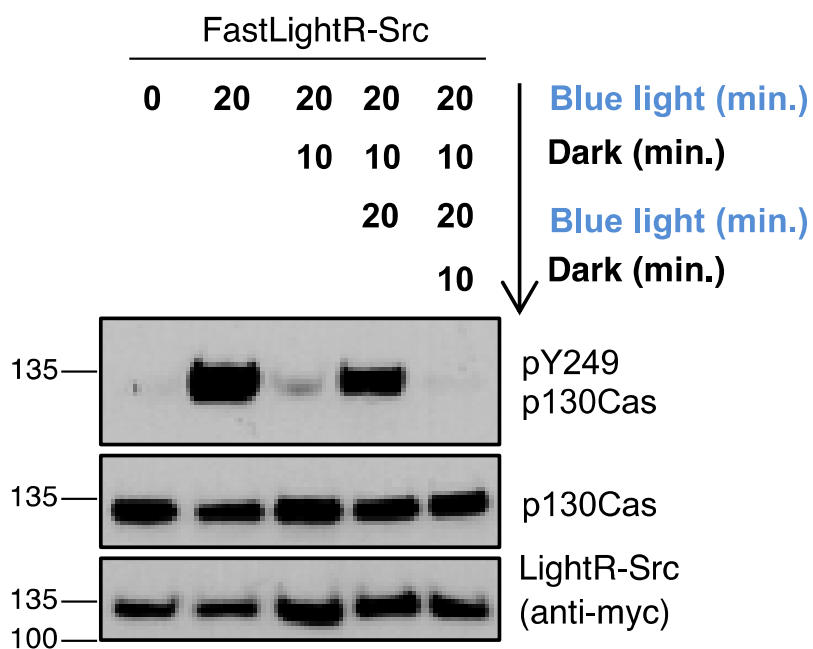


**Figure 18: Cycles of activation/inactivation of FastLightR-Src.** LinXE cells transiently expressing FastLightR-Src repeatedly incubated in the dark and in the light as indicated. Cell lysates were collected and probed for phosphorylation of Src substrate pY249 p130cas. All experiments were repeated at least 3 times with similar results.

### **G. LightR-Src Regulates Cell Morphology and Mimics Wild-type Src Localization**

Previous studies show that activation of Src leads to the stimulation of cell spreading<sup>29, 115-118</sup>. Therefore, we tested whether LightR-Src induces similar response in living cells. Our results show that cells expressing FastLightR-Src start spreading upon irradiation with blue light (Figure 19a) and stops immediately when the light is turned off. Repeated irradiation of cells with blue light induced corresponding cycles of cell spreading demonstrating again that LightR tool can be used to mimic oscillation of kinase activity in living cells (Figure 19a). Importantly, illumination of cells expressing catalytically inactive mutant of LightR-Src (D388R) did not induce any cell-spreading (Figure 19b).

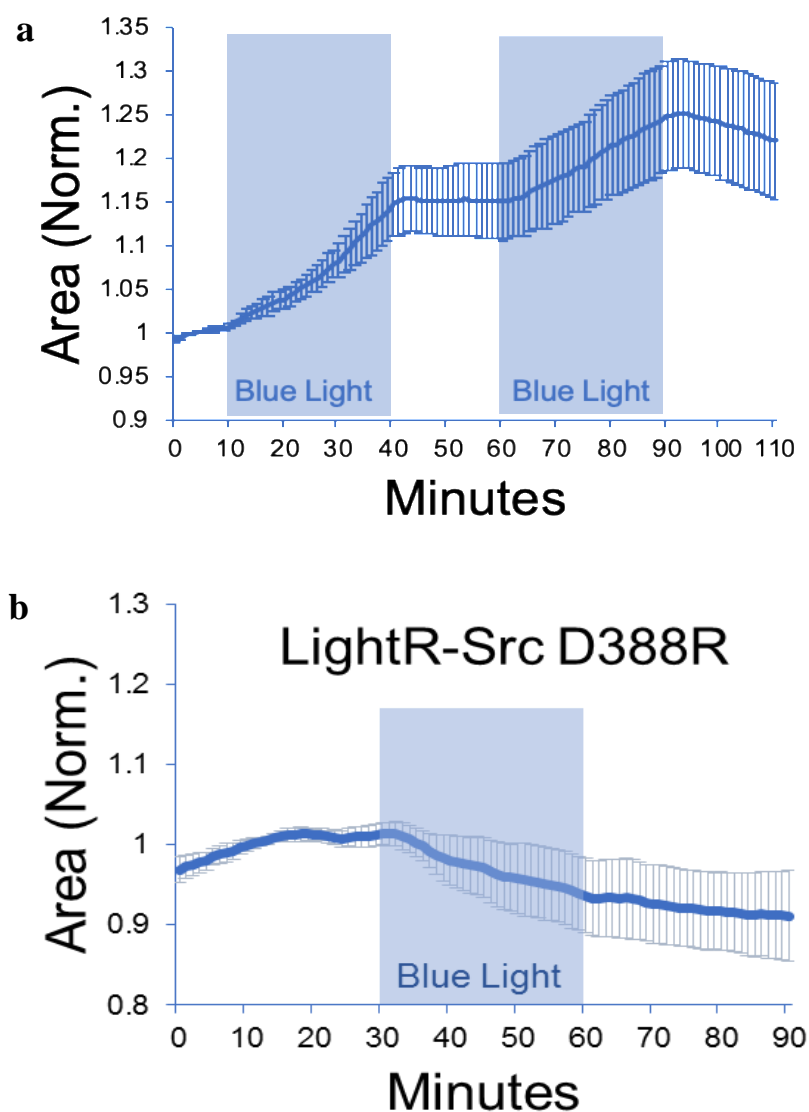


**Figure 19: Reversible and repetitive regulation of cell morphology by FastLightR-Src.** HeLa cells transiently co-expressing **a**, FastLightR-Src-mCherry (N = 11 cells) or **b**, catalytically inactive LightR-Src (D388R)-mCherry (N = 9 cells) with stargazin-iRFP670 (plasma membrane marker) were imaged live every minute while illuminated for the indicated periods of time (blue rectangles). Figures represent the quantification of changes in cell area. Graphs represent mean  $\pm$  90% confidence intervals.

Also, we observed that FastLightR-Src localizes in the perinuclear region in its inactive state and translocate to focal adhesions and cell membrane upon activation (Figure 20). This translocation is reversible and correlates with the activation/inactivation cycles of FastLightR-Src. Notably, this change in localization mimics that of wild type Src<sup>116, 119</sup>. Overall, our results demonstrate that LightR-Src can mediate cell morphodynamic changes and functions similarly to native Src kinase.

Dark → Blue light illumination, 30 min → Dark, 20 min → Blue light illumination, 30 min → Dark, 20 min

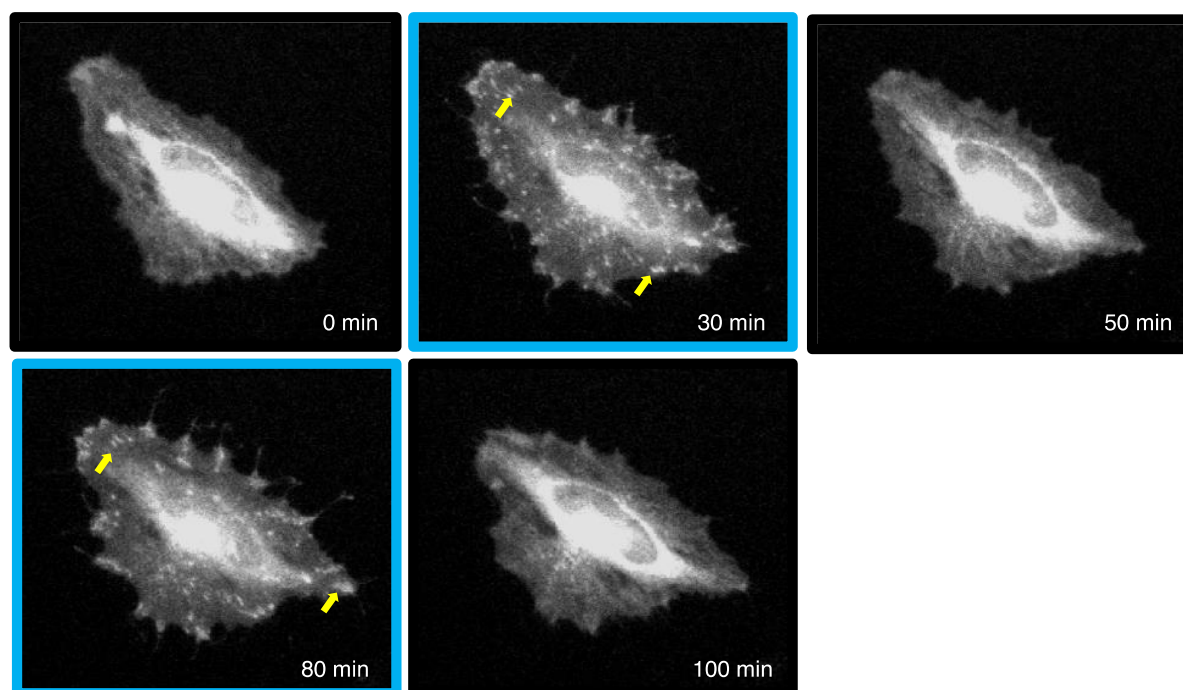
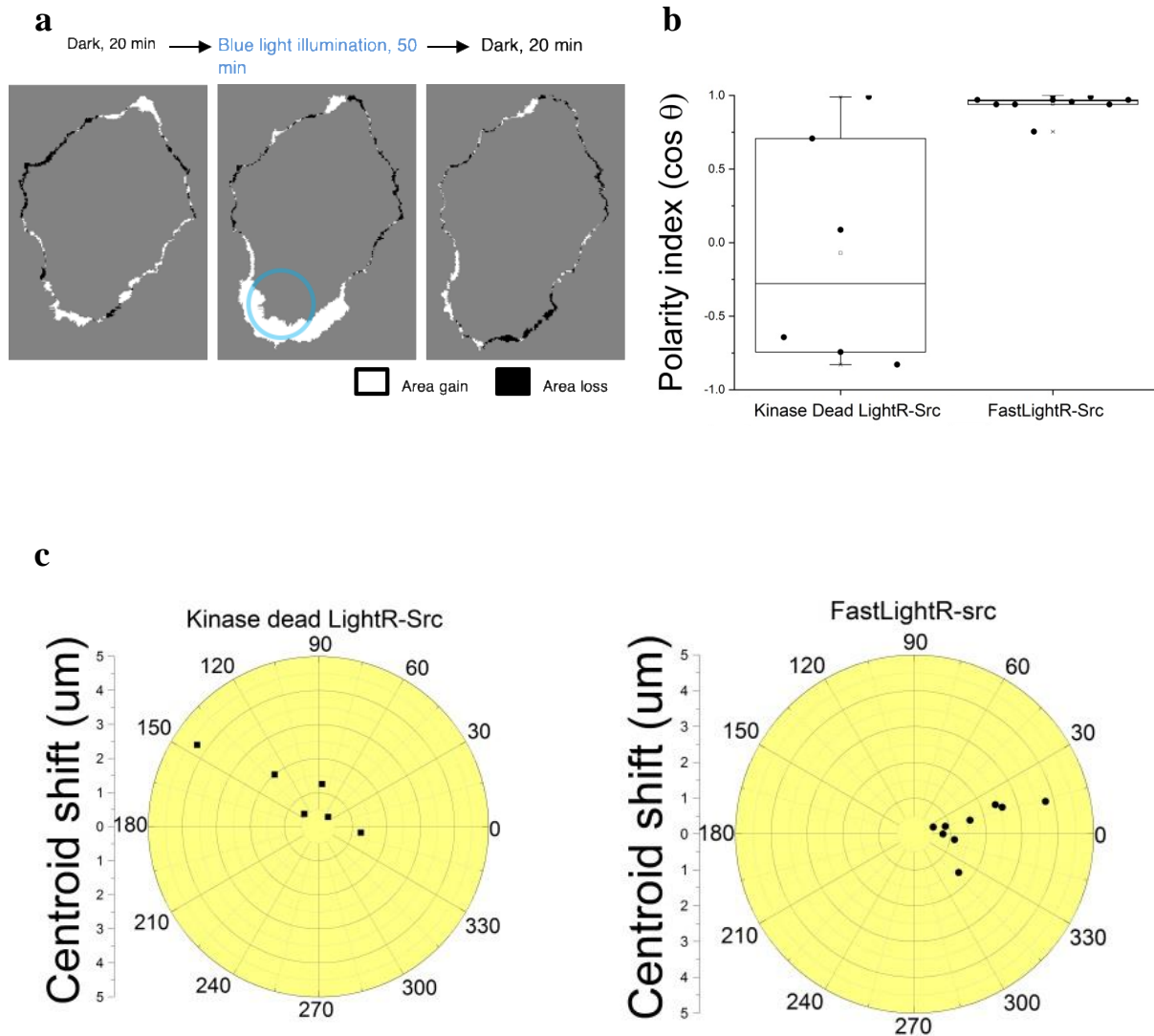


**Figure 20: Reversible and repetitive translocation of FastLightR-Src.** Representative images showing changes in LightR-Src localization upon illumination with blue light. Yellow arrows point to FastLightR-Src localization at structures resembling focal adhesions.

## **H. LightR-Src Activated at Subcellular Levels**

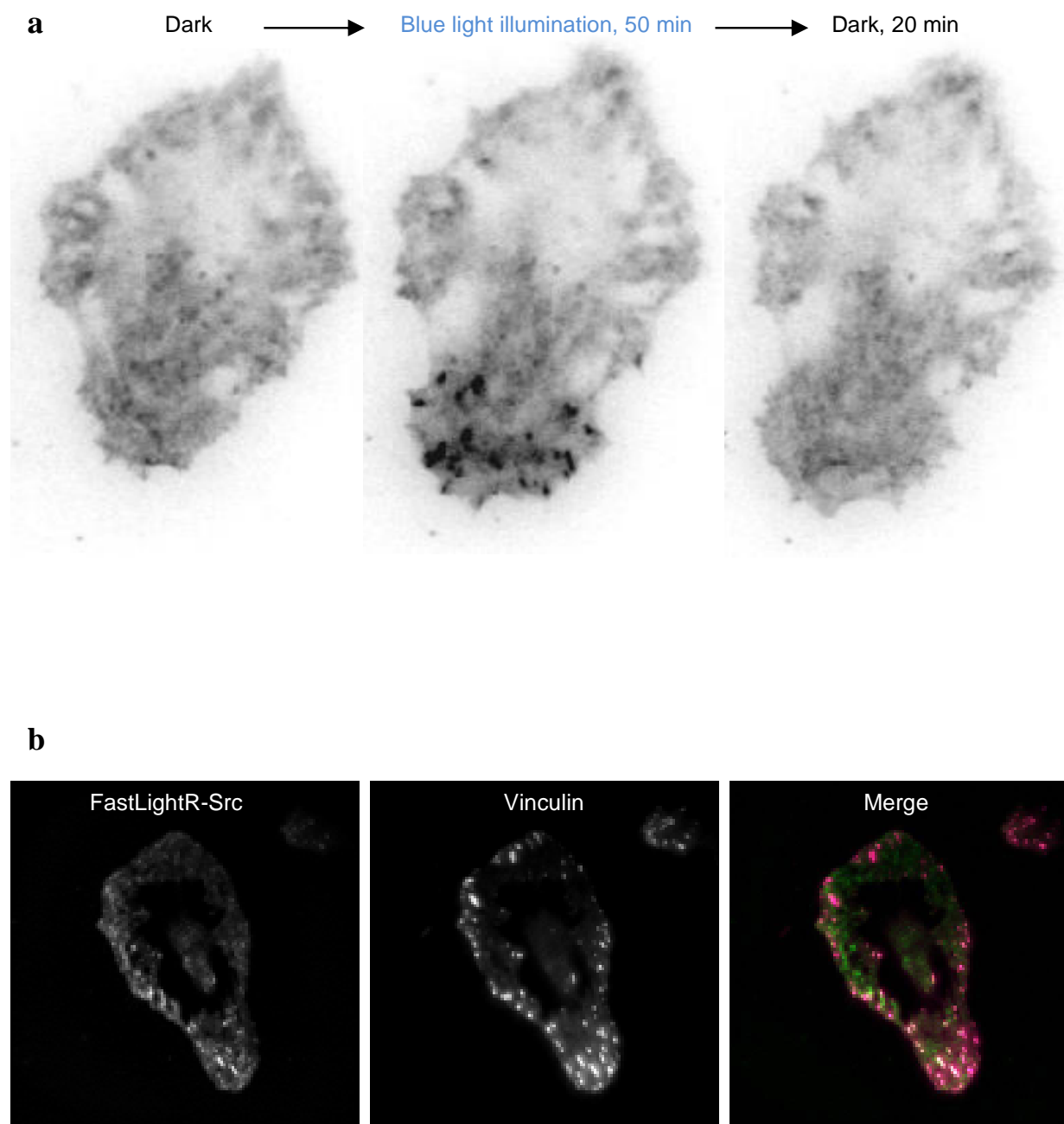
Localized activation of protein kinases is a critical determinant in the regulation of cell function. Previous studies suggested that local activation of Src at the cell periphery should stimulate the formation of local membrane protrusions<sup>117, 120</sup>. However, this hypothesis had indirect support and was not fully evaluated due to the limitations of existing methods. LightR approach on the other hand should allow us to define the effect of local activation of Src in living cells. To test this, we utilized FastLightR-Src construct that demonstrated fast off kinetics (Figure 17b). Local illumination of cells expressing FastLightR-Src induced formation of membrane protrusions proximal to the illuminated area and caused polarization of the cell towards the light (Figure 21a-c). This effect was reversed as soon as the light was switched off (Figure 21a). Cells expressing the catalytically inactive LightR-Src (D388R) did not polarize in response to local light irradiation (Figure 21b, c).





**Figure 21: Local regulation of FastLightR-Src at a subcellular level.** HeLa cells transiently co-expressing FastLightR-Src-mCherry and Stargazin-iRFP670 (plasma membrane marker) were imaged every minute and illuminated with blue light for indicated periods of time. **a**, Representative cell projection images showing protrusions formed between the indicated time points. Blue circle outlines illuminated area. **b**, Polarity index calculated for cells expressing catalytically inactive LightR-Src D388R (N = 6 cells) or FastLightR-Src (N = 10 cells). Box indicates the range percentile (25, 75); whiskers indicate the range outlier (1.5 Coef.) **c**, Polar plot for cells in **b** representing the centroid's migration distance and angle of deviation ( $\theta$ ) relative to local blue light illumination. Black dots represent individual cells.

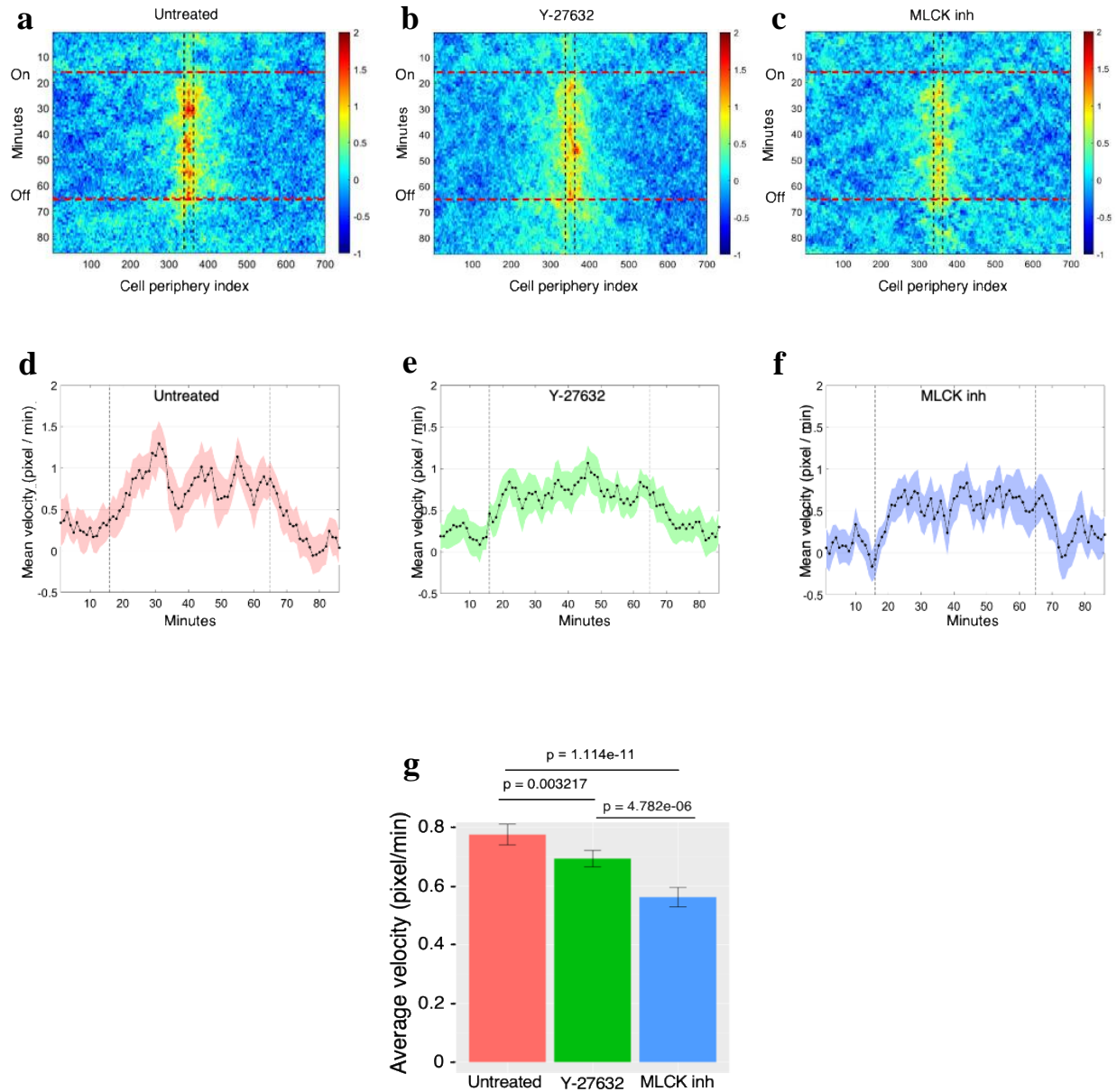
Notably, FastLightR-Src translocated to structures that resemble focal adhesions in the area illuminated with blue light and relocated back once the light was switched off (Figure 22a). To confirm that these structures are indeed focal adhesions, we co-expressed FastLightR-Src with Vinculin, a focal adhesion protein, and demonstrate their colocalization in the area of illumination with blue light (Figure 22b). This is again consistent with known activation-dependent changes in localization of wild type Src<sup>121, 122</sup>. These results reveal that local activation of Src is sufficient to induce local protrusions and demonstrate that LightR approach can be used for the regulation of kinase activity at subcellular levels.



**Figure 22: Local translocation of FastLightR-Src to focal adhesions.** **a**, Inverted contrast images of FastLightR-Src-mCherry acquired at the indicated time points. **b**, Images of a cell co-expressing FastLightR-Src-mCherry and Vinculin-Venus acquired using a total internal reflection fluorescence microscope (60X objective) after local exposure to blue light (area inside blue circle) for twenty-seven minutes. The merged image represents FastLightR-Src in green and Vinculin in magenta, with colocalization represented in white color and indicated with arrows.

## **I. Localized Src Activation Induces Waves of Membrane Protrusion**

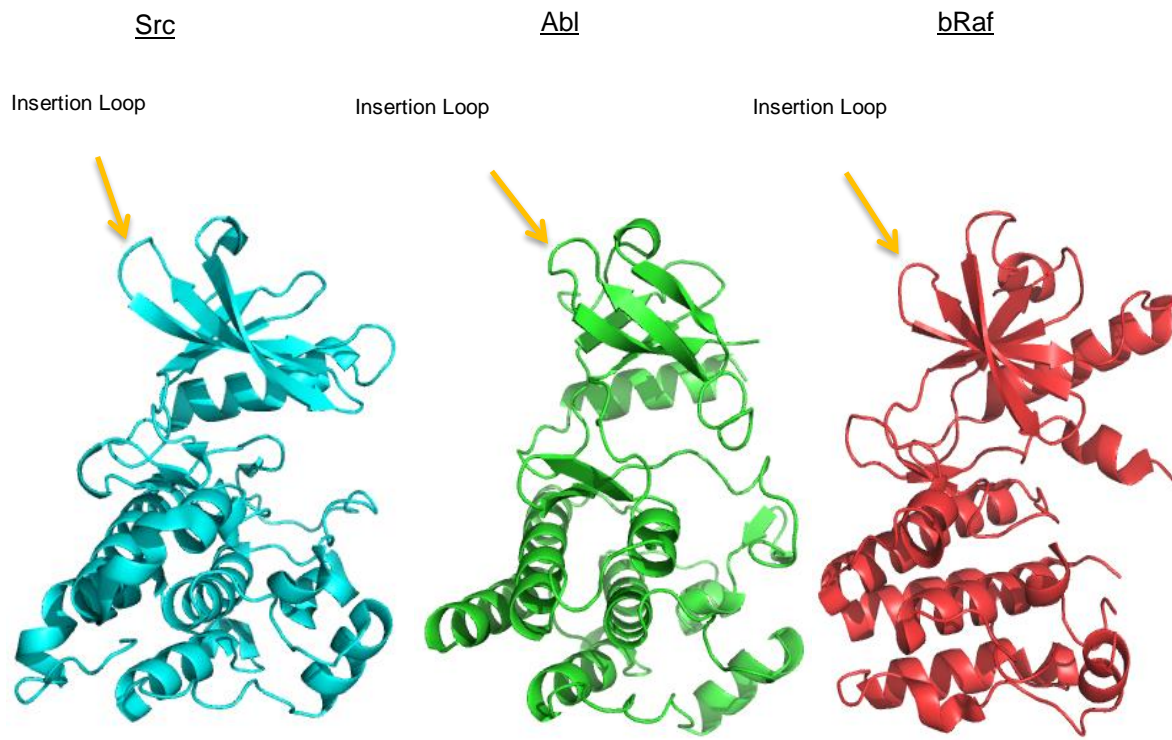
A previous study using a Src family kinases (SFK) biosensor suggested strong correlation between SFK activity at the cell periphery and cell-edge velocity <sup>123</sup>. LightR-Src allows us to determine the direct effect of local Src activity on protrusion dynamics. To achieve this, we evaluated temporal changes in cell edge velocity upon continuous local activation of LightR-Src. Our analysis revealed that Src induced local waves of increased cell-edge velocity (Figure 23a, d); suggesting the induction of recurrent local contractions that slow down membrane protrusion. Inhibition of Rho associate protein kinase (ROCK) and myosin light chain kinase (MLCK), major regulators of contractile machinery <sup>124, 125</sup>, perturbed these waves and reduced the average velocity of protrusions (Figure 23b, c, e-g). Interestingly, inhibition of ROCK caused significantly smaller average velocity reduction than inhibition of MLCK (Figure 23g), consistent with its limited role in phosphorylating MLC at the cell periphery <sup>126</sup>. Thus, our data demonstrate that sustained local Src activity induces waves of protrusions that are mediated by ROCK and MLCK.



**Figure 23: Localized Src activation induces waves of membrane protrusion.** Average cell-edge velocity kymograph for: **a**, untreated cells (N = 20 cells), **b**, cells pretreated with Y-27632 (10  $\mu$ M, N = 24 cells), or **c**, MLCK Inhibitor Peptide 18 (100  $\mu$ M, N = 20 cells). Vertical lines indicate the region illuminated with blue light. Horizontal lines indicate the time of blue light illumination. **d-f**, Mean velocity of the cell membrane region closest to the center of illumination spot. Vertical lines indicate the time of blue light illumination. Error bars represent 90% confidence interval. **g**, Average cell-edge velocity of figure 23 d-f during FastLightR-Src activation period. Error bars represent 90% confidence interval.

## **J. LightR Switch is Applicable to Other Kinases and Enzymes**

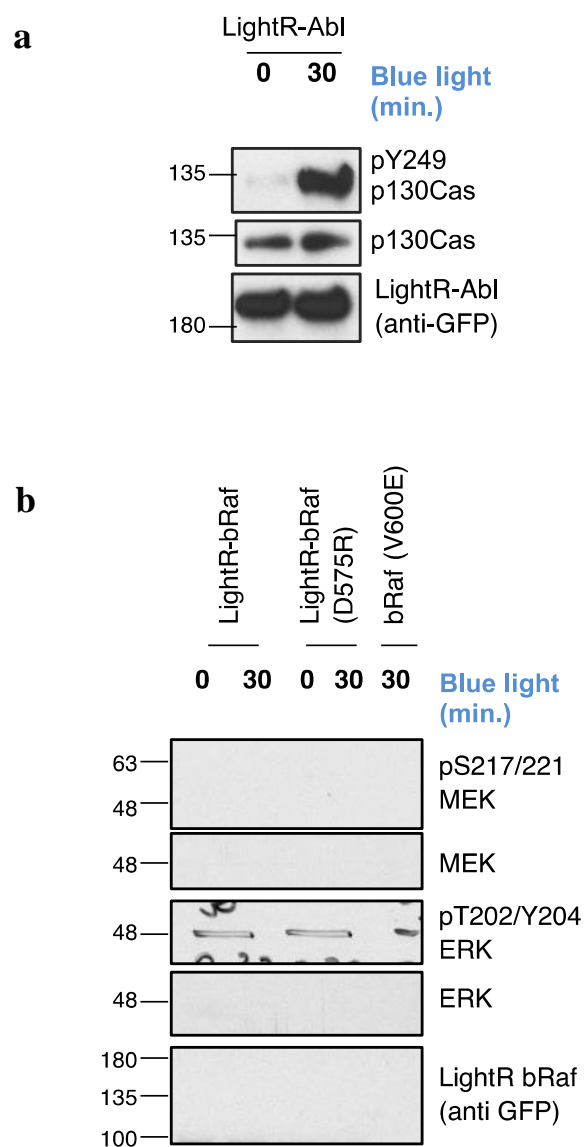
To verify that LightR approach is applicable to other kinases, we set out to engineer LightR variants of tyrosine kinase Abl and a dual specificity kinase b-Raf. Since majority of kinases share a conserved catalytic domain structure <sup>127</sup>, we inserted LightR switch in Abl and bRaf at a position analogous to the insertion site used in Src (Figure 24).



**Figure 24: Conserved catalytic domain of kinases.** Crystal structures of Src (PDB 1Y57), Abl (PDB 3CS9), and bRaf (PDB 4MNF) catalytic domains. Yellow arrows indicate LightR insertion site.

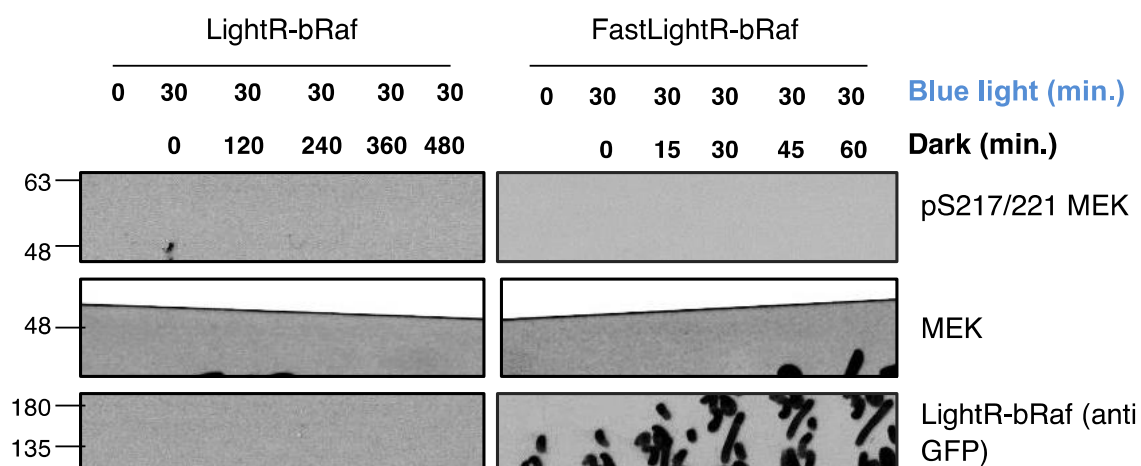
Our results show that illumination of cells expressing LightR-Abl induced the phosphorylation of known Abl substrate p130Cas (Figure 25a). Similarly, stimulation of LightR-bRaf induced phosphorylation of its direct target, MEK1, and led to downstream activation of ERK1 and ERK2 kinases (Figure 25b).





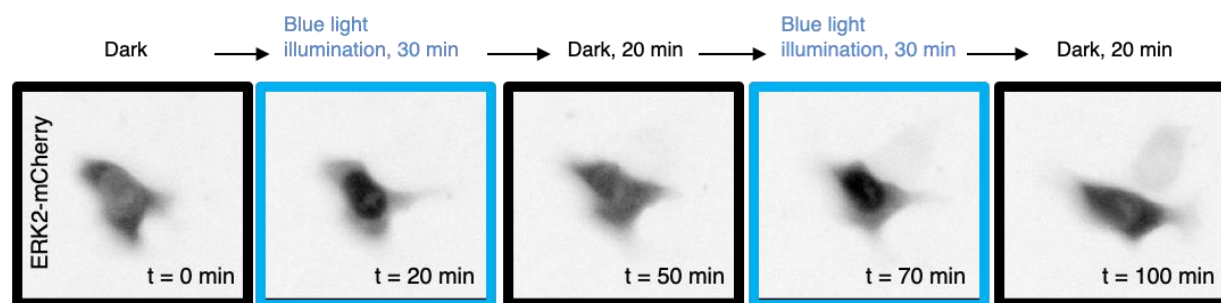
**Figure 25: Regulation of LightR-Abl and LightR-bRaf.** **a, b,** LinXE cells expressing the indicated kinase construct were continuously exposed to blue light for the specified period of time. Cell lysates were probed for the phosphorylation of the indicated proteins.

To demonstrate that LightR-bRaf off-kinetics are tunable, we generated a FastLightR-bRaf variant following the same strategy used to generate FastLightR-Src. This variant exhibited significantly faster deactivation kinetics compared to LightR-bRaf (Figure 26).



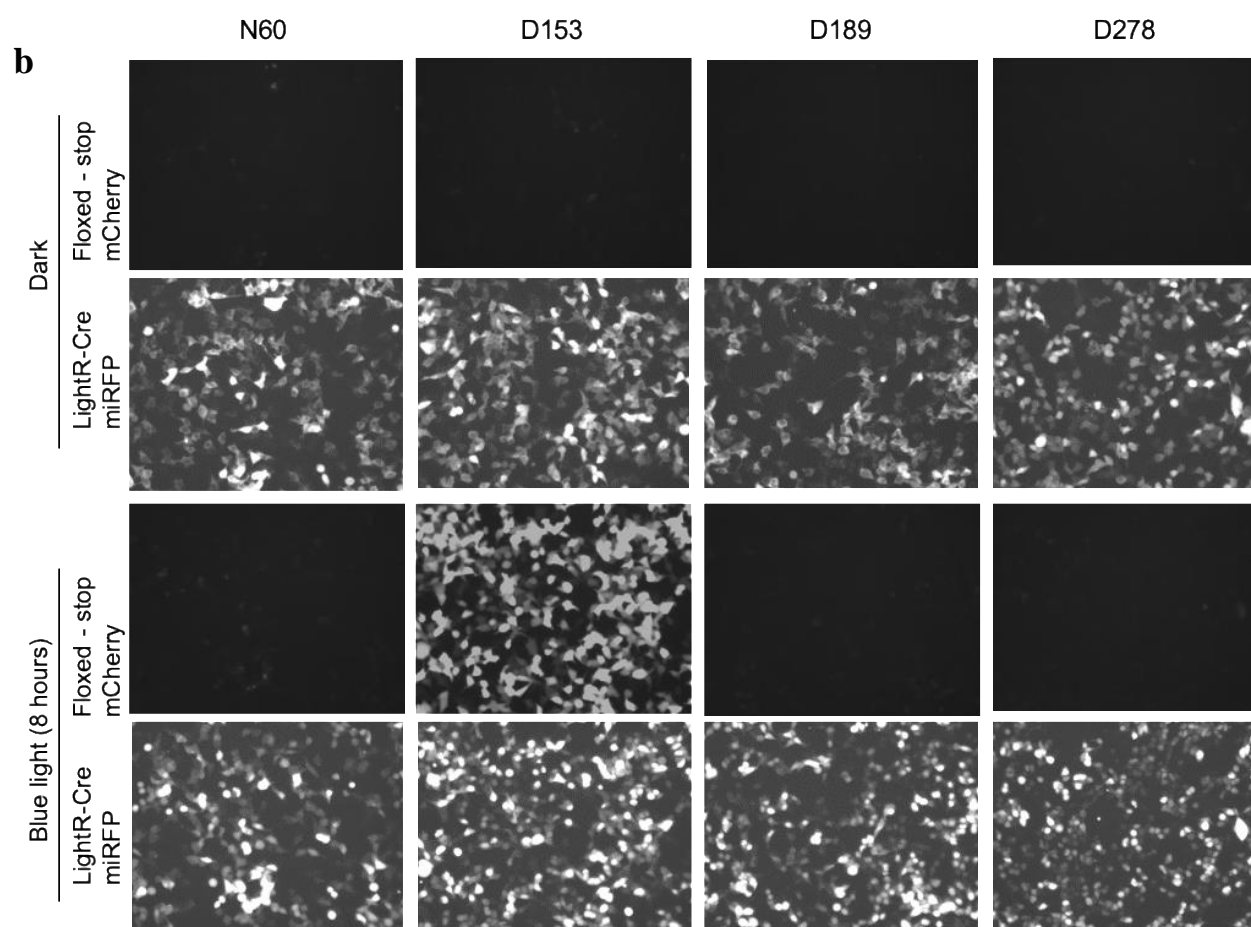
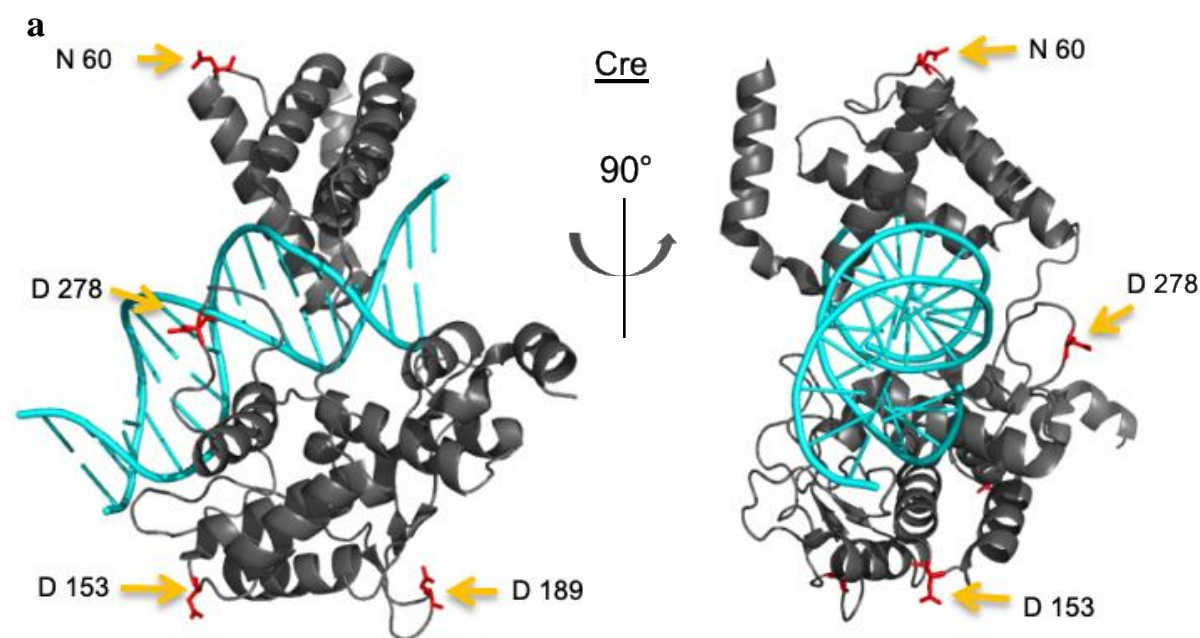
**Figure 26: Inactivation kinetics of LightR-bRaf and FastLightR-bRaf.** LinXE cells transiently expressing LightR-bRaf-venus or FastLightR-bRaf-venus variant were exposed to blue light for 30 minutes, and subsequently incubated in the dark for the indicated times. Cell lysates were probed for phosphorylation of MEK1 as indication of bRaf activity.

We also assessed if FastLightR-bRaf can undergo cyclic activation and deactivation by monitoring ERK2 kinase translocation into the nucleus, a known outcome of bRaf activation <sup>128</sup>. Indeed, ERK2 shuttles in and out of nucleus upon consecutive activation/inactivation cycles of FastLightR-bRaf (Figure 27). Overall, our data show that LightR approach can be applied to achieve light-mediated regulation of different protein kinases.



**Figure 27: Reversible and repetitive activation of FastLightR-bRaf.** LinXE cell transiently co-expressing FastLightR-bRaf-venus and ERK2-mCherry was imaged live while illuminated with blue light for two cycles. Representative images of ERK2-mCherry were taken at the indicated time points.

To demonstrate the broad applicability of LightR tool to other types of enzymes, we engineered LightR-Cre recombinase. We created four variants of Light-Cre that differ in their insertion site of LightR domain. The insertion sites are in four loops within Cre that are distant from the DNA binding site but connected to critical catalytic residues through an  $\alpha$ -helix (Figure 28a). The variant with LightR domain inserted at D153 residue showed activity in response to blue light (Figure 28b). This demonstrates that LightR approach can be used for regulation of different types of enzymes.



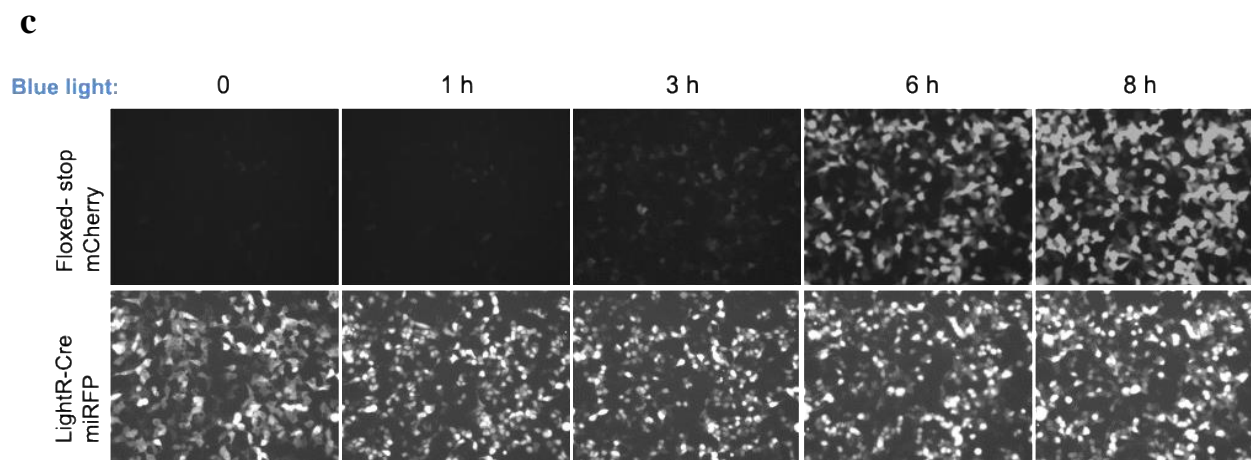


**Figure 28: LightR-Cre design and function.** **a**, Orthogonal view of Cre recombinase structure (PDB 1MA7) indicating LightR insertion sites (yellow arrows) of the 4 different LightR-Cre variants. **b**, LinXE cells transiently co-expressing floxed-stop-mCherry and one of LightR-Cre-miRFP variants were either kept in the dark or pulsed with blue light for 8 hours. The variants differ in their indicated insertion site (N60, D153, D189 or D278) of LightR domain in Cre recombinase, depicted in Figure 27a. **c**, LinXE cells transiently co-expressing floxed-stop-mCherry (upper panels) and LightR-Cre-miRFP (LightR inserted at D153, lower panels) were pulsed with blue light for the indicated times. All experiments were done at least 3 times with similar results.



## **V. DISCUSSION**

Our study describes an optogenetic approach that provides several advantages for interrogating signaling pathways. The regulation of protein activity is achieved via an allosteric control by inserting LightR switch in small loops in the protein's structure. Such approach provides flexibility in the selection of the insertion site and allows for specific regulation of the catalytic activity without interference with other functions of the protein such as interactions with binding partners <sup>16</sup>. Regulation by LightR domain is tunable, enabling different modes of regulation. LightR switch with slow off kinetics will be useful for long-term activation of LightR-enzymes since brief periodic pulses of light will be sufficient to maintain activity while avoiding phototoxicity caused by long exposure to blue light. Meanwhile, FastLightR switch will be suitable for studies that mimic transient, oscillatory or localized activation of a protein. It could also be used to study the kinetics of negative regulators of signaling pathways immediately after a signaling input is turned on. The activation of LightR-enzyme requires low intensity light; minimizing phototoxic effects of blue light illumination. Moreover, the regulation of LightR is limited to blue light, enabling its multiplexing with other red-shifted optogenetic tools or FRET biosensors. Finally, application of this tool to different classes of enzymes suggests its broad applicability for regulation of wide variety of protein functions in living cells.

Tight and efficient control of LightR allowed us to mimic fast signaling dynamics of Src kinase in cells and to establish stimulation of different signaling patterns over time. Several identified targets link early effects of Src activation to focal adhesion regulation and membrane protrusion formation. Our phosphoproteomics analysis reveals early Src-dependent phosphorylation of talin-1 at Y26 and Y70 residues (Figure 16a). These residues are located in the N-terminal F0 FERM domain of talin-1 <sup>129, 130</sup>. When talin-1 is in the inactive closed

conformation, F0 domain remains exposed and is proposed to act as an early detector of changes in the environment <sup>129</sup>. Thus, phosphorylation of talin-1 on Y26 and Y70 by Src may represent an early step in the inside-out integrin activation mechanism performed by talin <sup>131, 132</sup>. Later phosphorylation (1-5 min) of proteins involved in formation of new focal adhesions and membrane protrusions (such as lamellipodin, p130Cas, palladin, tensin-3, cortactin, GIT1, and paxillin) correlates with the time when we start detecting cell spreading (Figure 16b). Elevated phosphorylation of many proteins at 1 hour is indicative of oncogenic transformation processes mediated by prolonged activation of Src <sup>133, 134</sup>. Our phosphoproteomics studies also revealed that continuous Src activity induces only transient activation of MAP kinases ERK1 and ERK2 (Figure 16b). This suggests that short term Src activation induces activation of ERK1/2 whereas prolonged activity triggers inactivation of this pathway. Previous studies demonstrated that stimulation of cells with EGF results in transient activation of ERK1 and ERK2 <sup>135, 136</sup>. In the future studies, it will be interesting to determine if Src also plays a role in the negative regulation of ERK1/2 downstream of EGF.

The ability to regulate proteins on a subcellular level is one of the main capabilities desired in optogenetic tools. However, this has been challenging to achieve in methods employing steric hindrance and allosteric control as a mechanism of regulation <sup>12, 137</sup>. Efficiency and fast reversibility of FastLightR allowed us to control Src activity at specific location in the cell and demonstrate that its activity is sufficient to induce local protrusion. One of the interesting observations is the fact that continuous local activation of Src induces waves of protrusions instead of causing persistent protrusions (Figure 23a, d). Several groups have previously described periodic protrusions at the cell edge <sup>138-140</sup>, and correlated this phenotype with periodic contractions due to phosphorylation of myosin light chain (MLC) <sup>138-140</sup>. Our

results corroborate with these studies and demonstrate that both kinases that phosphorylate MLC (ROCK and MLCK) participate in the formation of the recurrent waves of protrusion in response to local Src activation. However, ROCK appears to be less important for maintaining overall elevated protrusion velocity downstream of Src activation (Figure 23g). Inhibition of MLCK resulted in much more noticeable reduction in average protrusion velocity (Figure 23g). Previous studies suggested that MLCK predominantly acts at the cell periphery where it mediates formation of stable protrusions and persistent migration of a cell <sup>126</sup>. Our data agrees with this function and suggest that MLCK is a predominant factor regulating cell protrusions downstream of Src. Future studies using LightR approach should determine the mechanism of this regulation.

## **VI. FUTURE DIRECTIONS**

This work introduced LightR tool, a method that regulates the activity of enzymes in cells using blue light. A new generation of LightR can be developed to respond to red-shifted wavelengths, by replacing the VVD photoreceptors with ones that respond to red light. This allows it to be more accessible in deep tissues and animal models, since red light is more penetrating than blue light. As an extension to this work, we can express LightR enzymes in animal models. This enables us to mimic pathological conditions of interest and study their progression from very early stages. For instance, Src and bRaf are highly transforming oncoproteins, therefore LightR-Src and LightR-bRaf can be used to induce cancer in animal models at a specific time and location to study early molecular and morphological changes a normal tissue undergoes during transformation in a native environment.

LightR approach can be further engineered to dissect signaling pathways. By tagging it with a light-activated dimer component, we can simultaneously activate LightR and induce its interaction with a binding partner that is also tagged with another light activated dimer component. For instance, if protein-X is known to activate protein-Y and protein-Z, using this approach, we can study the effect of LightR-X activation of protein-Y only, but not protein-Z, and vice versa.

An interesting concept that could be investigated with this tool is whether acute activation of LightR-Src, or any other enzyme of interest, induces long term or permanent changes to its downstream effectors, and whether these changes require certain threshold of activity that should be met by the enzyme. Studies similar to the phosphoproteomics analysis

presented here could be performed to answer this question since it detects global and broad changes downstream of activation.

## **VII. CITED LITERATURE**

1. Lee, M.J. and M.B. Yaffe, *Protein Regulation in Signal Transduction*. Cold Spring Harb Perspect Biol, 2016. **8**(6).
2. Bugaj, L.J., et al., *Cancer mutations and targeted drugs can disrupt dynamic signal encoding by the Ras-Erk pathway*. Science, 2018. **361**(6405).
3. Cohen-Saidon, C., et al., *Dynamics and variability of ERK2 response to EGF in individual living cells*. Mol Cell, 2009. **36**(5): p. 885-93.
4. Marshall, C.J., *Specificity of receptor tyrosine kinase signaling: transient versus sustained extracellular signal-regulated kinase activation*. Cell, 1995. **80**(2): p. 179-85.
5. Rauch, N., et al., *MAPK kinase signalling dynamics regulate cell fate decisions and drug resistance*. Curr Opin Struct Biol, 2016. **41**: p. 151-158.
6. Guntas, G., et al., *Engineering an improved light-induced dimer (iLID) for controlling the localization and activity of signaling proteins*. Proc Natl Acad Sci U S A, 2015. **112**(1): p. 112-7.
7. Wang, H., et al., *LOVTRAP: an optogenetic system for photoinduced protein dissociation*. Nat Methods, 2016. **13**(9): p. 755-8.
8. Strickland, D., et al., *TULIPs: tunable, light-controlled interacting protein tags for cell biology*. Nat Methods, 2012. **9**(4): p. 379-84.
9. Kawano, F., et al., *Engineered pairs of distinct photoswitches for optogenetic control of cellular proteins*. Nature Communications, 2015. **6**(1): p. 6256.
10. Wang, J., et al., *Time-resolved protein activation by proximal decaging in living systems*. Nature, 2019. **569**(7757): p. 509-513.
11. Dagliyan, O., et al., *Engineering extrinsic disorder to control protein activity in living cells*. Science, 2016. **354**(6318): p. 1441-1444.
12. Zhou, X.X., et al., *Optical control of cell signaling by single-chain photoswitchable kinases*. Science, 2017. **355**(6327): p. 836-842.
13. Diaz, J.E., et al., *A Split-Abl Kinase for Direct Activation in Cells*. Cell Chem Biol, 2017. **24**(10): p. 1250-1258.e4.
14. Wu, Y.I., et al., *A genetically encoded photoactivatable Rac controls the motility of living cells*. Nature, 2009. **461**(7260): p. 104-108.
15. Hongdusit, A., et al., *Minimally disruptive optical control of protein tyrosine phosphatase 1B*. Nat Commun, 2020. **11**(1): p. 788.
16. Karginov, A.V., et al., *Engineered allosteric activation of kinases in living cells*. Nature Biotechnology, 2010. **28**(7): p. 743-747.
17. Winkler, A., et al., *Structural Details of Light Activation of the LOV2-based Photoswitch PA-Rac1*. ACS Chemical Biology, 2015. **10**(2): p. 502-509.

18. Toettcher, J.E., O.D. Weiner, and W.A. Lim, *Using optogenetics to interrogate the dynamic control of signal transmission by the Ras/Erk module*. Cell, 2013. **155**(6): p. 1422-34.
19. Toettcher, J.E., et al., *The promise of optogenetics in cell biology: interrogating molecular circuits in space and time*. Nat Methods, 2011. **8**(1): p. 35-8.
20. Chang, K.-Y., et al., *Light-inducible receptor tyrosine kinases that regulate neurotrophin signalling*. Nature Communications, 2014. **5**(1): p. 4057.
21. Grusch, M., et al., *Spatio-temporally precise activation of engineered receptor tyrosine kinases by light*. The EMBO Journal, 2014. **33**(15): p. 1713-1726.
22. Kim, N., et al., *Spatiotemporal Control of Fibroblast Growth Factor Receptor Signals by Blue Light*. Chemistry & Biology, 2014. **21**(7): p. 903-912.
23. Wend, S., et al., *Optogenetic Control of Protein Kinase Activity in Mammalian Cells*. ACS Synthetic Biology, 2014. **3**(5): p. 280-285.
24. Boyden, E.S., *Optogenetics and the future of neuroscience*. Nat Neurosci, 2015. **18**(9): p. 1200-1.
25. Deisseroth, K., *Optogenetics: 10 years of microbial opsins in neuroscience*. Nat Neurosci, 2015. **18**(9): p. 1213-25.
26. Ziegler, T. and A. Möglich, *Photoreceptor engineering*. Frontiers in Molecular Biosciences, 2015. **2**(30).
27. Uda, Y., et al., *Efficient synthesis of phycocyanobilin in mammalian cells for optogenetic control of cell signaling*. Proceedings of the National Academy of Sciences, 2017. **114**(45): p. 11962.
28. Kholodenko, B.N., *Cell-signalling dynamics in time and space*. Nature Reviews Molecular Cell Biology, 2006. **7**(3): p. 165-176.
29. Karginov, A.V., et al., *Dissecting motility signaling through activation of specific Src-effector complexes*. Nat Chem Biol, 2014. **10**(4): p. 286-90.
30. Karunarathne, W.K., P.R. O'Neill, and N. Gautam, *Subcellular optogenetics - controlling signaling and single-cell behavior*. J Cell Sci, 2015. **128**(1): p. 15-25.
31. Benedetti, L., et al., *Light-activated protein interaction with high spatial subcellular confinement*. Proceedings of the National Academy of Sciences, 2018. **115**(10): p. E2238-E2245.
32. Beyer, H.M., et al., *Optogenetic control of signaling in mammalian cells*. Biotechnol J, 2015. **10**(2): p. 273-83.
33. Buckley, C.E., et al., *Reversible Optogenetic Control of Subcellular Protein Localization in a Live Vertebrate Embryo*. Dev Cell, 2016. **36**(1): p. 117-126.
34. Horner, M., et al., *Optogenetic control of focal adhesion kinase signaling*. Cell Signal, 2018. **42**: p. 176-183.

35. Xu, Y., et al., *Optogenetic activation reveals distinct roles of PI<sub>3</sub> and Akt in adipocyte insulin action*. Journal of Cell Science, 2016. **129**(10): p. 2085.
36. Idevall-Hagren, O., et al., *Optogenetic control of phosphoinositide metabolism*. Proc Natl Acad Sci U S A, 2012. **109**(35): p. E2316-23.
37. Levskaya, A., et al., *Spatiotemporal control of cell signalling using a light-switchable protein interaction*. Nature, 2009. **461**(7266): p. 997-1001.
38. Valon, L., et al., *Optogenetic control of cellular forces and mechanotransduction*. Nat Commun, 2017. **8**: p. 14396.
39. Zimmerman, S.P., et al., *Cells lay their own tracks – optogenetic Cdc42 activation stimulates fibronectin deposition supporting directed migration*. Journal of Cell Science, 2017. **130**(18): p. 2971.
40. O'Banion, C.P., et al., *Design and Profiling of a Subcellular Targeted Optogenetic cAMP-Dependent Protein Kinase*. Cell Chem Biol, 2018. **25**(1): p. 100-109.e8.
41. Muhlhauser, W.W.D., W. Weber, and G. Radziwill, *OpEn-Tag-A Customizable Optogenetic Toolbox To Dissect Subcellular Signaling*. ACS Synth Biol, 2019. **8**(7): p. 1679-1684.
42. O'Neill, P.R. and N. Gautam, *Subcellular optogenetic inhibition of G proteins generates signaling gradients and cell migration*. Mol Biol Cell, 2014. **25**(15): p. 2305-14.
43. de Beco, S., et al., *Optogenetic dissection of Rac1 and Cdc42 gradient shaping*. Nature Communications, 2018. **9**(1): p. 4816.
44. Yoo, S.K., et al., *Differential Regulation of Protrusion and Polarity by PI(3)K during Neutrophil Motility in Live Zebrafish*. Developmental Cell, 2010. **18**(2): p. 226-236.
45. Graziano, B.R., et al., *A module for Rac temporal signal integration revealed with optogenetics*. J Cell Biol, 2017. **216**(8): p. 2515-2531.
46. Leung, D.W., et al., *Genetically encoded photoswitching of actin assembly through the Cdc42-WASP-Arp2/3 complex pathway*. Proc Natl Acad Sci U S A, 2008. **105**(35): p. 12797-802.
47. Bugaj, L.J., et al., *Optogenetic protein clustering and signaling activation in mammalian cells*. Nat Methods, 2013. **10**(3): p. 249-52.
48. Bugaj, L.J., et al., *Regulation of endogenous transmembrane receptors through optogenetic Cry2 clustering*. Nat Commun, 2015. **6**: p. 6898.
49. Chatelle, C.V., et al., *Optogenetically controlled RAF to characterize BRAF and CRAF protein kinase inhibitors*. Sci Rep, 2016. **6**: p. 23713.
50. Nguyen, M.K., et al., *Optogenetic oligomerization of Rab GTPases regulates intracellular membrane trafficking*. Nature Chemical Biology, 2016. **12**(6): p. 431-436.
51. Richards, F.M., *ON THE ENZYMIC ACTIVITY OF SUBTILISIN-MODIFIED RIBONUCLEASE*. Proc Natl Acad Sci U S A, 1958. **44**(2): p. 162-6.



52. Ullmann, A., F. Jacob, and J. Monod, *Characterization by in vitro complementation of a peptide corresponding to an operator-proximal segment of the beta-galactosidase structural gene of Escherichia coli*. J Mol Biol, 1967. **24**(2): p. 339-43.
53. Villarejo, M., P.J. Zamenhof, and I. Zabin, *Beta-galactosidase. In vivo -complementation*. J Biol Chem, 1972. **247**(7): p. 2212-6.
54. Luker, K.E., et al., *Kinetics of regulated protein-protein interactions revealed with firefly luciferase complementation imaging in cells and living animals*. Proc Natl Acad Sci U S A, 2004. **101**(33): p. 12288-93.
55. Pelletier, J.N., F.X. Campbell-Valois, and S.W. Michnick, *Oligomerization domain-directed reassembly of active dihydrofolate reductase from rationally designed fragments*. Proc Natl Acad Sci U S A, 1998. **95**(21): p. 12141-6.
56. Wehrman, T., et al., *Protein-protein interactions monitored in mammalian cells via complementation of beta -lactamase enzyme fragments*. Proc Natl Acad Sci U S A, 2002. **99**(6): p. 3469-74.
57. Wilson, C.G., T.J. Magliery, and L. Regan, *Detecting protein-protein interactions with GFP-fragment reassembly*. Nat Methods, 2004. **1**(3): p. 255-62.
58. Shekhawat, S.S. and I. Ghosh, *Split-protein systems: beyond binary protein-protein interactions*. Curr Opin Chem Biol, 2011. **15**(6): p. 789-97.
59. Konermann, S., et al., *Optical control of mammalian endogenous transcription and epigenetic states*. Nature, 2013. **500**(7463): p. 472-476.
60. Polstein, L.R. and C.A. Gersbach, *A light-inducible CRISPR-Cas9 system for control of endogenous gene activation*. Nat Chem Biol, 2015. **11**(3): p. 198-200.
61. Wang, X., X. Chen, and Y. Yang, *Spatiotemporal control of gene expression by a light-switchable transgene system*. Nat Methods, 2012. **9**(3): p. 266-9.
62. Polstein, L.R. and C.A. Gersbach, *Light-inducible spatiotemporal control of gene activation by customizable zinc finger transcription factors*. J Am Chem Soc, 2012. **134**(40): p. 16480-3.
63. Taslimi, A., et al., *Optimized second-generation CRY2-CIB dimerizers and photoactivatable Cre recombinase*. Nat Chem Biol, 2016. **12**(6): p. 425-30.
64. Meador, K., et al., *Achieving tight control of a photoactivatable Cre recombinase gene switch: new design strategies and functional characterization in mammalian cells and rodent*. Nucleic Acids Res, 2019. **47**(17): p. e97.
65. Kawano, F., et al., *A photoactivatable Cre-loxP recombination system for optogenetic genome engineering*. Nat Chem Biol, 2016. **12**(12): p. 1059-1064.
66. Nihongaki, Y., et al., *Photoactivatable CRISPR-Cas9 for optogenetic genome editing*. Nature Biotechnology, 2015. **33**(7): p. 755-760.
67. Nihongaki, Y., et al., *A split CRISPR-Cpf1 platform for inducible genome editing and gene activation*. Nature Chemical Biology, 2019. **15**(9): p. 882-888.
68. Yu, D., et al., *Optogenetic activation of intracellular antibodies for direct modulation of endogenous proteins*. Nature Methods, 2019. **16**(11): p. 1095-1100.

69. Shimizu-Sato, S., et al., *A light-switchable gene promoter system*. Nat Biotechnol, 2002. **20**(10): p. 1041-4.
70. Muller, K., et al., *A red/far-red light-responsive bi-stable toggle switch to control gene expression in mammalian cells*. Nucleic Acids Res, 2013. **41**(7): p. e77.
71. Dagliyan, O., et al., *Computational design of chemogenetic and optogenetic split proteins*. Nature Communications, 2018. **9**(1): p. 4042.
72. Huse, M. and J. Kuriyan, *The conformational plasticity of protein kinases*. Cell, 2002. **109**(3): p. 275-82.
73. Lee, J., et al., *Surface sites for engineering allosteric control in proteins*. Science, 2008. **322**(5900): p. 438-42.
74. Dagliyan, O., N.V. Dokholyan, and K.M. Hahn, *Engineering proteins for allosteric control by light or ligands*. Nature Protocols, 2019. **14**(6): p. 1863-1883.
75. Dagliyan, O., et al., *Engineering extrinsic disorder to control protein activity in living cells*. Science, 2016. **354**: p. 1441-1444.
76. Karginov, A.V., et al., *Engineered allosteric activation of kinases in living cells*. Nat Biotechnol, 2010. **28**(7): p. 743-7.
77. Han, T., Q. Chen, and H. Liu, *Engineered Photoactivatable Genetic Switches Based on the Bacterium Phage T7 RNA Polymerase*. ACS Synthetic Biology, 2017. **6**(2): p. 357-366.
78. Strickland, D., K. Moffat, and T.R. Sosnick, *Light-activated DNA binding in a designed allosteric protein*. Proceedings of the National Academy of Sciences, 2008. **105**: p. 10709-10714.
79. Niopek, D., et al., *Engineering light-inducible nuclear localization signals for precise spatiotemporal control of protein dynamics in living cells*. Nature Communications, 2014. **5**(1): p. 4404.
80. Yumerefendi, H., et al., *Control of Protein Activity and Cell Fate Specification via Light-Mediated Nuclear Translocation*. PLoS One, 2015. **10**(6): p. e0128443.
81. Niopek, D., et al., *Optogenetic control of nuclear protein export*. Nature Communications, 2016. **7**(1): p. 10624.
82. Yumerefendi, H., et al., *Light-induced nuclear export reveals rapid dynamics of epigenetic modifications*. Nat Chem Biol, 2016. **12**(6): p. 399-401.
83. Niopek, D., et al., *Engineering light-inducible nuclear localization signals for precise spatiotemporal control of protein dynamics in living cells*. Nat Commun, 2014. **5**: p. 4404.
84. Yi, J.J., et al., *Manipulation of endogenous kinase activity in living cells using photoswitchable inhibitory peptides*. ACS synthetic biology, 2014. **3**(11): p. 788-795.
85. Lungu, O.I., et al., *Designing photoswitchable peptides using the AsLOV2 domain*. Chemistry & biology, 2012. **19**(4): p. 507-517.

86. Bongor, K.M., et al., *General method for regulating protein stability with light*. ACS Chem Biol, 2014. **9**(1): p. 111-5.
87. Usherenko, S., et al., *Photo-sensitive degron variants for tuning protein stability by light*. BMC systems biology, 2014. **8**: p. 128-128.
88. Zhou, X.X., et al., *Optical control of cell signaling by single-chain photoswitchable kinases*. Science, 2017. **355**(6327): p. 836.
89. Stone, O.J., et al., *Optogenetic control of cofilin and  $\alpha$ TAT in living cells using Z-lock*. Nat Chem Biol, 2019. **15**(12): p. 1183-1190.
90. Pettersen, E.F., et al., *UCSF Chimera--a visualization system for exploratory research and analysis*. J Comput Chem, 2004. **25**(13): p. 1605-12.
91. Sali, A. and T.L. Blundell, *Comparative protein modelling by satisfaction of spatial restraints*. J Mol Biol, 1993. **234**(3): p. 779-815.
92. Phillips, J.C., et al., *Scalable molecular dynamics with NAMD*. J Comput Chem, 2005. **26**(16): p. 1781-802.
93. Bakan, A., L.M. Meireles, and I. Bahar, *ProDy: protein dynamics inferred from theory and experiments*. Bioinformatics, 2011. **27**(11): p. 1575-7.
94. Cai, X., et al., *Spatial and temporal regulation of focal adhesion kinase activity in living cells*. Mol Cell Biol, 2008. **28**(1): p. 201-14.
95. Dittmann, A., et al., *High-fat diet in a mouse insulin-resistant model induces widespread rewiring of the phosphotyrosine signaling network*. Mol Syst Biol, 2019. **15**(8): p. e8849.
96. Mou, Y., et al., *Engineering Improved Antiphosphotyrosine Antibodies Based on an Immunoconvergent Binding Motif*. Journal of the American Chemical Society, 2018. **140**(48): p. 16615-16624.
97. Szklarczyk, D., et al., *STRING v11: protein-protein association networks with increased coverage, supporting functional discovery in genome-wide experimental datasets*. Nucleic Acids Res, 2019. **47**(D1): p. D607-d613.
98. Tsygankov, D., et al., *CellGeo: a computational platform for the analysis of shape changes in cells with complex geometries*. The Journal of cell biology, 2014. **204**(3): p. 443-460.
99. Zhurikhina, A., et al., *EdgeProps: A Computational Platform for Correlative Analysis of Cell Dynamics and Near-Edge Protein Activity*. Methods in molecular biology (Clifton, N.J.), 2018. **1821**: p. 47-56.
100. Nihongaki, Y., et al., *Genetically engineered photoinducible homodimerization system with improved dimer-forming efficiency*. ACS Chem Biol, 2014. **9**(3): p. 617-21.
101. Vaidya, A.T., et al., *Structure of a light-activated LOV protein dimer that regulates transcription*. Sci Signal, 2011. **4**(184): p. ra50.
102. Zoltowski, B.D. and B.R. Crane, *Light activation of the LOV protein vivid generates a rapidly exchanging dimer*. Biochemistry, 2008. **47**(27): p. 7012-9.

103. Zoltowski, B.D., et al., *Conformational switching in the fungal light sensor Vivid*. Science, 2007. **316**(5827): p. 1054-7.
104. Cowan-Jacob, S.W., *Structural biology of protein tyrosine kinases*. Cellular and Molecular Life Sciences CMLS, 2006. **63**(22): p. 2608-2625.
105. Krupa, A., G. Preethi, and N. Srinivasan, *Structural modes of stabilization of permissive phosphorylation sites in protein kinases: distinct strategies in Ser/Thr and Tyr kinases*. Journal of molecular biology, 2004. **339**(5): p. 1025-1039.
106. Zheng, X.M., R.J. Resnick, and D. Shalloway, *A phosphotyrosine displacement mechanism for activation of Src by PTPalpha*. Embo j, 2000. **19**(5): p. 964-78.
107. Cunningham-Edmondson, A.C. and S.K. Hanks, *p130Cas substrate domain signaling promotes migration, invasion, and survival of estrogen receptor-negative breast cancer cells*. Breast cancer (Dove Medical Press), 2009. **1**: p. 39-52.
108. Sachdev, S., Y. Bu, and I.H. Gelman, *Paxillin-Y118 phosphorylation contributes to the control of Src-induced anchorage-independent growth by FAK and adhesion*. BMC cancer, 2009. **9**: p. 12-12.
109. Cargnello, M. and P.P. Roux, *Activation and function of the MAPKs and their substrates, the MAPK-activated protein kinases*. Microbiol Mol Biol Rev, 2011. **75**(1): p. 50-83.
110. Zoltowski, B.D., B. Vaccaro, and B.R. Crane, *Mechanism-based tuning of a LOV domain photoreceptor*. Nature chemical biology, 2009. **5**(11): p. 827-834.
111. Purvis, Jeremy E. and G. Lahav, *Encoding and Decoding Cellular Information through Signaling Dynamics*. Cell, 2013. **152**(5): p. 945-956.
112. Conlon, P., et al., *Single-cell dynamics and variability of MAPK activity in a yeast differentiation pathway*. Proceedings of the National Academy of Sciences, 2016. **113**(40): p. E5896.
113. Li, Y., et al., *Mitogen-activated protein kinase (MAPK) dynamics determine cell fate in the yeast mating response*. The Journal of biological chemistry, 2017. **292**(50): p. 20354-20361.
114. Zhang, Q., et al., *Visualizing Dynamics of Cell Signaling In Vivo with a Phase Separation-Based Kinase Reporter*. Molecular Cell, 2018. **69**(2): p. 334-346.e4.
115. Klomp, J.E., et al., *Mimicking transient activation of protein kinases in living cells*. Proc Natl Acad Sci U S A, 2016. **113**(52): p. 14976-14981.
116. Kaplan, K.B., et al., *c-Src enhances the spreading of src-/- fibroblasts on fibronectin by a kinase-independent mechanism*. Genes Dev, 1995. **9**(12): p. 1505-17.
117. Cary, L.A., et al., *Src Catalytic but Not Scaffolding Function Is Needed for Integrin-Regulated Tyrosine Phosphorylation, Cell Migration, and Cell Spreading*. Molecular and Cellular Biology, 2002. **22**(8): p. 2427.
118. Fu, P., et al., *Sphingolipids Signaling in Lamellipodia Formation and Enhancement of Endothelial Barrier Function*. Curr Top Membr, 2018. **82**: p. 1-31.

119. Chu, P.-H., et al., *Engineered kinase activation reveals unique morphodynamic phenotypes and associated trafficking for Src family isoforms*. Proceedings of the National Academy of Sciences, 2014. **111**(34): p. 12420-12425.
120. Baumgartner, M., et al., *c-Src-Mediated Epithelial Cell Migration and Invasion Regulated by PDZ Binding Site*. Molecular and Cellular Biology, 2008. **28**(2): p. 642.
121. Dhar, A. and S.D. Shukla, *Involvement of pp60c-src in platelet-activating factor-stimulated platelets. Evidence for translocation from cytosol to membrane*. J Biol Chem, 1991. **266**(28): p. 18797-801.
122. Weernink, P.A. and G. Rijksen, *Activation and translocation of c-Src to the cytoskeleton by both platelet-derived growth factor and epidermal growth factor*. J Biol Chem, 1995. **270**(5): p. 2264-7.
123. Gulyani, A., et al., *A biosensor generated via high-throughput screening quantifies cell edge Src dynamics*. Nat Chem Biol, 2011. **7**(7): p. 437-44.
124. Parri, M., et al., *EphrinA1 activates a Src/focal adhesion kinase-mediated motility response leading to rho-dependent actino/myosin contractility*. J Biol Chem, 2007. **282**(27): p. 19619-28.
125. Totsukawa, G., et al., *Distinct roles of ROCK (Rho-kinase) and MLCK in spatial regulation of MLC phosphorylation for assembly of stress fibers and focal adhesions in 3T3 fibroblasts*. J Cell Biol, 2000. **150**(4): p. 797-806.
126. Totsukawa, G., et al., *Distinct roles of MLCK and ROCK in the regulation of membrane protrusions and focal adhesion dynamics during cell migration of fibroblasts*. J Cell Biol, 2004. **164**(3): p. 427-39.
127. Fabbro, D., S.W. Cowan-Jacob, and H. Moebitz, *Ten things you should know about protein kinases: IUPHAR Review 14*. Br J Pharmacol, 2015. **172**(11): p. 2675-700.
128. Burack, W.R. and A.S. Shaw, *Live Cell Imaging of ERK and MEK: simple binding equilibrium explains the regulated nucleocytoplasmic distribution of ERK*. J Biol Chem, 2005. **280**(5): p. 3832-7.
129. Bouaouina, M., Y. Lad, and D.A. Calderwood, *The N-terminal domains of talin cooperate with the phosphotyrosine binding-like domain to activate beta1 and beta3 integrins*. J Biol Chem, 2008. **283**(10): p. 6118-25.
130. Goult, B.T., et al., *Structure of a double ubiquitin-like domain in the talin head: a role in integrin activation*. Embo j, 2010. **29**(6): p. 1069-80.
131. Vinogradova, O., et al., *A Structural Mechanism of Integrin  $\alpha$ IIb $\beta$ 3 "Inside-Out" Activation as Regulated by Its Cytoplasmic Face*. Cell, 2002. **110**(5): p. 587-597.
132. Vinogradova, O., et al., *Membrane-mediated structural transitions at the cytoplasmic face during integrin activation*. Proc Natl Acad Sci U S A, 2004. **101**(12): p. 4094-9.
133. Hunter, T. and B.M. Sefton, *Transforming gene product of Rous sarcoma virus phosphorylates tyrosine*. Proc Natl Acad Sci U S A, 1980. **77**(3): p. 1311-5.
134. Sefton, B.M., et al., *Evidence that the phosphorylation of tyrosine is essential for cellular transformation by Rous sarcoma virus*. Cell, 1980. **20**(3): p. 807-16.

135. Olsen, J.V., et al., *Global, in vivo, and site-specific phosphorylation dynamics in signaling networks*. Cell, 2006. **127**(3): p. 635-48.
136. Sasagawa, S., et al., *Prediction and validation of the distinct dynamics of transient and sustained ERK activation*. Nature Cell Biology, 2005. **7**(4): p. 365-373.
137. Dagliyan, O., et al., *Engineering extrinsic disorder to control protein activity in living cells*. Science (New York, N.Y.), 2016. **354**(6318): p. 1441-1444.
138. Tsai, F.C. and T. Meyer, *Ca<sup>2+</sup> pulses control local cycles of lamellipodia retraction and adhesion along the front of migrating cells*. Curr Biol, 2012. **22**(9): p. 837-42.
139. Giannone, G., et al., *Periodic Lamellipodial Contractions Correlate with Rearward Actin Waves*. Cell, 2004. **116**(3): p. 431-443.
140. Machacek, M. and G. Danuser, *Morphodynamic profiling of protrusion phenotypes*. Biophysical journal, 2006. **90**(4): p. 1439-1452.

## VIII. APPENDIX

The American Physiological Society allows the reuse for text and figures of published articles without permission.

Below is a screen shot from the American Physiological Society website:  
<https://journals.physiology.org/author-info.permissions>

## Copyright and Permissions

### Reuse by Authors of Their Work Published by APS

---

### Reuse by Non-authors of APS Published Content

---

### Reuse in APS Publications of non-APS Published Content

---

## Reuse by Authors of Their Work Published by APS

The APS Journals are copyrighted for the protection of authors and the Society. The Mandatory Submission Form serves as the Society's official copyright transfer form. Author's rights to reuse their APS-published work are described below:

Republication in New Works	Authors may republish parts of their final-published work (e.g., figures, tables), without charge and without requesting permission, provided that full citation of the source is given in the new work.
Meeting Presentations and Conferences	Authors may use their work (in whole or in part) for presentations (e.g., at meetings and conferences). These presentations may be reproduced on any type of media in materials arising from the meeting or conference such as the proceedings of a meeting or conference. A copyright fee will apply if there is a charge to the user or if the materials arising are directly or indirectly commercially supported <sup>1</sup> . Full citation is required.
Theses and Dissertations	Authors may reproduce whole published articles in dissertations and post to thesis repositories without charge and without requesting permission. Full citation is required.

### **VIII. APPENDIX (continued)**

The journal of eLife permits unrestricted use for text and figures of papers published in their journal for a thesis or dissertation.

Below is a screen shot from eLife website: <https://reviewer.elifesciences.org/author-guide/journal-faqs>

**9. Can I use text, figures, and tables from the paper I published in eLife in a thesis or dissertation?**

Yes, you can. Please include a reference to the eLife paper and include a statement to say that the eLife article is distributed under the terms of a [Creative Commons Attribution](#) that permits unrestricted use and redistribution provided that the original author and source are credited.



## **IX. VITA**

Name	Mark Shaaya
Education	Ph.D. Cellular and Molecular Pharmacology, University of Illinois at Chicago (UIC), Chicago, IL. To be conferred 2020  B.Sc. Biochemistry, Lebanese University, Lebanon. 2008
Honors	Woeltjen Poster Award. 2017 & 2018  Honorable mention in College of Medicine 2017 Research forum. 2017  ASCB/EMBO travel award. 2016  ASPET travel award. 2016  CCTS/PECTS Pre-doctoral Education for Clinical and Translational Scientists Fellowship. 2016  Murphy's fellowship. 2016  Best group at Quantitative Fluorescence Microscopy course. 2016  CSCTR travel award. 2016  UIC Graduate Student Council Travel Award. 2016  National Institutes of Health (NIH) Lung Biology and Pathobiology Training Grant. 2014 & 2015
Professional Membership	American Society for Biochemistry and Molecular Biology. 2017  American Society for Pharmacology and Experimental Therapeutics. 2016 - 2018.  American Society for Cell Biology. 2015 - 2018  American Thoracic Society. 2015 – 2016  American Heart Association 2015 - 2017

## **IX. VITA (continued)**

Publications **Shaaya M**, Fauser J, Zhurikhina A, Conage-Pough JE, Huyot V, Brennan M, Flower CT, Matsche J, Khan S, Natarajan V, Rehman J, Kota P, White FM, Tsygankov D, Karginov AV. LightR: A Light-Regulated Allosteric Switch Enables Temporal and Subcellular Control of Enzyme Activity. *eLife*. 2020 (in revisions).

**Shaaya M**, Fauser J, Karginov AV. Optogenetics, the art of Illuminating complex signaling pathways. *Physiology*, 2020 (accepted).

Fu P, Ramchandran R, **Shaaya M**, Huang L, Ebenezer DL, Jiang Y, Komarova Y, Vogel SM, Malik AB, Minshall RD, Du G, Tonks NK, Natarajan V. Phospholipase D2 restores endothelial barrier function by promoting PTPN14-mediated VE-cadherin dephosphorylation. *J Biol Chem*. 2020. PMID: 32327488

Klomp JE, **Shaaya M**, Matsche J, Rebiai R, Aaron JS, Collins KB, Huyot V, Gonzalez AM, Muller WA, Chew TL, Malik AB, Karginov AV. Time-Variant SRC Kinase Activation Determines Endothelial Permeability Response. *Cell Chem Biol*. 2019. PMID: 31130521

Suryadevara V, Huang L, Kim SJ, Cheresh P, **Shaaya M**, Bandela M, Fu P, Feghali-Bostwick C, Di Paolo G, Kamp DW, Natarajan V. Role of phospholipase D in bleomycin-induced mitochondrial reactive oxygen species generation, mitochondrial DNA damage, and pulmonary fibrosis. *Am J Physiol Lung Cell Mol Physiol*. 2019. PMID: 31090437

Fu P, **Shaaya M**, Harijith A, Jacobson JR, Karginov A, Natarajan V. Sphingolipids Signaling in Lamellipodia Formation and Enhancement of Endothelial Barrier Function. *Curr Top Membr*. 2018. PMID: 30360778

Fu P, Ebenezer DL, Berdyshev EV, Bronova IA, **Shaaya M**, Harijith A, Natarajan V. Role of Sphingosine Kinase 1 and S1P Transporter Spns2 in HGF-mediated Lamellipodia Formation in Lung Endothelium. *J Biol Chem*. 2016. PMID: 27864331

**IX. VITA (continued)**

Teaching      Teaching Assistant, GCLS 515: Receptor Pharmacology and Cell Signaling.  
UIC-Chicago, IL. 2018 - 2019

Teaching Assistant, GCLS 503: Cell Biology. UIC-Chicago, IL. 2015 - 2016

Selected      Experimental Biology conference, (abstract # 533.101). 2018

talks          American Society of Cell Biology Conference, (abstract # 8010). 2017

GEMS Research Symposium, UIC Chicago. 2017